Investigations of Stabilization of Cr in Spinel Phase in Chromium-Containing Slags

Galina Jelkina Albertsson

Licentiate Thesis

Stockholm 2011

Division of Materials Process Science
Department of Material Science and Engineering
Royal Institute of Technology
SE-10044 Stockholm
Sweden

Akademisk avhandling som med tillstånd av Kungliga Tekniska Högskolan i Stockholm, framlägges för offentlig granskning för avläggande av Teknologie Licentiatexamen, fredagen den 16 december 2011, kl 10.00 i sal B23, Brinellvägen 23, Kungliga Tekniska Högskolan, Stockholm

---

ISRN KTH/MSE--11/43--SE+THMETU/AVH
ISBN 978-91-7501-207-0

Galina Jelkina Albertsson, *Investigations of Stabilization of Cr in Spinel Phase in Chromium-Containing Slags*

KTH School of Industrial Engineering and Management
Division of Materials Process Science
Royal Institute of Technology
SE-10044 Stockholm
Sweden

ISRN KTH/MSE--11/43--SE+THMETU/AVH
ISBN 978-91-7501-207-0

Abstract

The influence of basicity, heat treatment as well as different oxygen partial pressures on the phase relationships in the CaO-MgO-SiO_2-Cr_2O_3 slags was studied with a view to control the precipitation of Cr-spinel in the slag phase. The equilibrium phases in CaO-MgO-SiO_2-Cr_2O_3 slag system in the range on 1673-1873 K have been investigated under low oxygen partial pressure as well as in as air atmosphere. In low oxygen partial pressure experiments, a suitable mixture of CO and CO_2 was used to control the oxygen partial pressure. The oxygen partial pressure was kept at 10^{-4} Pa. The Cr_2O_3 and MgO contents in the slag were fixed to be 6 and 8wt% respectively. The basicity (CaO/ SiO_2) of the slag was varied in the range 1.0-2.0. Gas/slag equilibrium technique was adopted to synthesize the slag at a suitable temperature above the liquidus point. One heat treatment procedure is that the samples were heated to and soaked at 1873 K for 24h in order to achieve the equilibrium state and subsequently quenched in water. The other is that the samples were heated to and soaked at 1873 K for 24h, then slow cooled to 1673 K and soaked at this temperature for additional 24h in order to achieve the equilibrium state at lower temperature before quenching in water. The chromium distribution and phase compositions in the quenched slag were studied using scanning electron microscopy (SEM), energy dispersive spectroscopy (EDS) and X-ray diffraction techniques (XRD). FACTsage software was used for the phase equilibrium calculations. The experimental results obtained from the present work are compared with the calculation results from FACTsage software as well as with results from samples directly quenched after soaking at 1873K. It is found that the spinel formation at 1873 K in air atmosphere is favored in the slag basicity range of 1.0 to 1.6. The size of spinel crystals increased drastically after slow cooling followed by annealing compared to samples being quenched after soaking at 1873 K. The amount of foreign elements dissolved in the spinel phase, and matrix phases decreased after slow cooling followed by annealing at lower temperature, resulting in purer phases with less defects. It was found that the amount of foreign elements in the spinel phase, and other phases decreased after soaking at very low P_{O2}. The size of the spinel crystals was found to be larger in samples with low basicity. Spinel phase precipitation has improved in the samples with higher basicities compared to the results obtained in air.

Keywords: Cr_2O_3 containing slags; gas-slag equilibrium; chromium partition; spinel;

Acknowledgements

First of all, I would like to express my sincere gratitude and appreciation to my supervisors, Docent Lidong Teng and Professor Seshadri Seetharaman, for giving me the opportunity to join the group in the Division of Materials Process Science at Royal Institute of Technology and for the guidance and support during my study. This work is carried out in close cooperation with Luleå technical university, Sweden. The author would like to thank Professor Bo Björkman and Dr Fredrik Engström for the valuable discussions and suggestions during the work and the preparation of the manuscript. Financial support for the project from Swedish Foundation for Strategic Environmental Research (MISTRA-88035) through Jernkontoret, Sweden is gratefully acknowledged. My thanks to Ms. Wenli Long, Ms. Fang Mei and Ms. Anastasiia Riazanova for their help during the SEM-EDS. I would like to acknowledge Mr. Peter Kling for his excellent technical support and offering tea and goodies during my study. I am also very grateful to all colleagues and friends in MSE for their kind help and support. Finally, I wish to thank all my loved ones, my thoughts are always with you.

Galina Jelkina

November 2011, Stockholm, Sweden

Supplements

The present thesis is based on the following supplements:

Supplement 1: "Effect of basicity on the chromium partition in CaO-MgO-SiO_2-Cr_2O_3 synthetic slag at 1873 K"

Galina Jelkina, Lidong Teng, Bo Björkman

Submitted to Metallurgical and Materials Transactions B for publication

Supplement 2: "Effect of the heat treatment on the chromium partition in CaO-MgO-SiO_2-Cr_2O_3 synthetic slags"

Galina Jelkina, Lidong Teng, Seshadri Seetharaman

Supplement 3: "Effect of the oxygen partial pressure on the chromium partition in CaO-MgO-SiO_2-Cr_2O_3 synthetic slag at 1673 K"

Galina Jelkina

The contribution by the author to the different supplements of the thesis:

1. Literature survey, experimental work, thermodynamic calculations, major part of the writing.
2. Literature survey, experimental work, thermodynamic calculations, major part of the writing.
3. Literature survey, experimental work, thermodynamic calculations, major part of the writing.

Contents

Chapter 1

Introduction

Significant amounts of chromium-containing slags are annually produced by the steelmaking companies in Sweden and other countries all over the world. These slags are generally accumulated in landfill areas during the past decades of steel production. Leaching of chromium and other heavy metals from the slag deposits is a main environmental problem that has to be solved. Metallurgical slag waste from stainless steel production process containing environmentally harmful elements, such as chromium, is a continuously growing problem. A number of mineralogical phases present in the slag matrix can dissolve chromium and lead to chromium leaching in water. Chromium in slag if not stabilized, could oxidize to the hexavalent state (Cr^{6+}), and thus leach out if exposed to acidic and oxygen rich environment[1, 2]. Utilization of chromium containing steelmaking slag is thus restricted. Recently, elution behaviour of elements from chromium containing phases into seawater was investigated by Samada et al. It was found that the existence of dicalcium silicate enhanced the dissolution of chromium into seawater [3]. Ca_2SiO_4 is also strongly dissolved by acidified water, while wüstite appear to be resistant[4]. In order to avoid the presence of Ca_2SiO_4, some attempts have been made to modify the slag composition, for example by decreasing the slag basicity[3 ,4]. However, low basicity slags cause rapid refractory degradation and low chromium yields [5 ,6]. Thus, the slag composition must be adjusted after slag/metal separation [7]. Presence of free CaO and MgO as well as merwinite phase is also undesirable in view of their water solubility. Merwinite is considered as being soluble throughout the entire pH range. Thus, chromium dissolved in merwinite, CaO and MgO can easily end up in water [1-8]. Adding relatively large amount of silica, for example quartz sand or waste glass, is one way to control the slag composition and prevent slag disintegration [3-8].

Mineralogical phases considered in the current work, are divided into spinel, monoxide solid solution and the silicate matrix phases.

Magnesiochromite spinel phase ($MgCr_2O_4$) is known to be important for controlling the leaching properties of chromium from the slag[1, 2]. The results of earlier works are generally in agreement that activity of chromium is strongly decreased in magnesiochromite spinel because of the strong bonding of chromium in the spinel. $MgCr_2O_4$ is thus very stable towards oxidation and is resistant to dissolution [1-2, 9-14]. It might be possible to increase the slag stability by increasing the spinel phase content by means of controlled solidification of the

slag. The leaching of chromium from the slag is expected to be low or negligible if the chromium is bound to the $MgCr_2O_4$ or $FeCr_2O_4$ spinel phase[1]. Mineralogical phases present in a slag system are highly dependent on slag composition and heat treatment history[1-2, 8, 15-16].

In slags, chromium can be present in different valence states, the most common ones being Cr^{2+} and Cr^{3+}. Results from the earlier work by Wang and Seetharaman[17] indicate that the ratio of $X_{CrO}/X_{CrO1.5}$ in CaO-SiO_2-CrOx and CaO-MgO-(FeO-) Al_2O_3-SiO_2-CrOx slags systems increases with the increasing temperature and decreasing oxygen partial pressure, while the slag basicity tends to decrease the ratio up to a certain level beyond which, the ratio is unaffected by basicity. This indicates that, in order to stabilize the spinel phase in slags, the treatment conditions must be strictly controlled. There are discrepancies in literature regarding the influence of the composition and basicity of slag on the spinel precipitation from Cr-containing slags [1, 3, 9]. When the formation of a phase is thermodynamically favoured, the dimensions of the crystals will depend on the temperature to which the crystals are exposed and the duration of the exposure[1].

Pre-calculated phase diagrams by FACTsage give an indication that, for the slag systems within the basicity range of 1.0 to 1.5, the treatment temperature can be decreased to approximately 1673 K. Fast cooling from 1873 K must be avoided due to the high Cr solubility in the matrix phases at higher temperatures. The slags of interest for this work are stainless steelmaking slags both from EAF and AOD processes, since they contain relatively large amounts of chromium and other alloying elements with well-defined conditions such as oxygen pressures, slag basicities and heat treatment conditions.

Discrepancies[1-10] in the results from the previous studies regarding the effect of cooling rate on the phase distribution as well as a lack of an efficient method of spinel phase precipitation in metallurgical slag requires further investigation. Tossavainen et al [15] studied the influence of rapid cooling by water granulation and its effect on chromium leachability. The differences between granulated slag samples and conventional slag were low. Lonchar et al [16] studied the effect of the cooling rate on hot EAF slag on the leaching behavior. It was concluded that the cooling method has a significant effect on the leaching behavior of slags.

Numerous mineralogical phases present in steelmaking slags are soluble in aqueous media, as for example, merwinite, periclase, dicalcium silicate and lime. Other phases present in the slags, *viz.* wüstite, spinel and glass are, on other hand, considered as resistant to dissolution.

While the wüstite and glass formation were studied by earlier researchers [1-12], very little effort has been made towards an understanding of the precipitation of spinel phase in the slag.

Most part of the stainless steel is produced in AOD (Argon Oxygen Decarburization) often combined with EAF (Electric Arc Furnace) processes. In the AOD process, the gas formed during the decarburization operation is continuously diluted by argon gas in order to decrease the partial pressure of P_{O_2}. By this method, the carbon in the stainless steel can be removed efficiently without excessive chromium oxidation[18]. The partial oxygen pressures in the AOD and EAF processes after slag reduction thus in general within the range of 10^{-4}-10^{-2} Pa. Very little experimental effort has been made towards an understanding of the precipitation of spinel phase in the slag at low oxygen partial pressures. Thus, the present work is intended for finding an approach for the optimum precipitation of the spinel crystals and their growth in the slag by means of controlled reaction gas atmosphere.

The slags of interest for this work are stainless steelmaking slags both from EAF and AOD processes, since they contain relatively large amounts of chromium. The aim is to study the chromium partition in the slag and get an understanding of the phase relationships in the CaO-MgO-SiO_2-Cr_2O_3 slags with a view to control the precipitation of Cr-spinel in the slag phase. In order to achieve this aim, the classical gas/slag equilibrium method was adopted in the present study for the synthesis of the slag samples with well-defined conditions such as oxygen pressure, slag basicities and heat treatment conditions. To the knowledge of the present authors, no systematic investigation has been carried out regarding the conditions of precipitation of spinel phase in the slag.

Slow cooling and soaking sequences as well as well-controlled oxygen partial pressures are applied in this work in order to keep the system close to equilibrium, so that the equilibrium phases could be studied. The chromium distribution and phase composition were studied using SEM, EDS and XRD techniques in synthetic slags at a fixed MgO and Cr_2O_3 contents. The experimental results obtained from the present work are compared with the calculation results from FACTsage software[19].

Chapter 2

Theoretical Background

2.1 Thermodynamic calculations

The equilibrium phases of CaO-MgO-SiO_2 -Cr_2O_3 slag system with various basicities at 1673 K and oxygen partial pressure $P_{O_2}=10^{-4}$ Pa were calculated by FACTsage software (FACTsage6.1), Thermfact Ltd (Montreal, Canada) and BTT-technologies (Aachen, Germany). Databases chosen were Fact53 and FToxid. Equilibrium phase amounts are presented in Table 1 along with the calculated results conducted for air as atmosphere (in brackets). These calculation results will be compared with the current experimental results in the section of discussions.

Figure 1 shows an isotherm for the CaO-MgO-SiO_2 -Cr_2O_3 system at 1673 K in air. Figure 2 shows an isotherm for the CaO-MgO-SiO_2 -Cr_2O_3 system at 1673 K and oxygen partial pressure $P_{O_2}=10^{-4}$ Pa. Figure 3 shows an isopleth section for the CaO-MgO-SiO_2 -Cr_2O_3 system with the oxygen partial pressure fixed to $P_{O_2}=10^{-4}$ Pa. The Cr_2O_3 and MgO contents are set to 6 wt% and 8wt% respectively. The compositions of the slags investigated in the current work are marked in the figures 1-3.

Table 1 Amounts of equilibrium phases in mass percent at 1673 K and oxygen partial pressure $P_{O_2}=10^{-4}$ Pa, results from the thermodynamic calculations by FACTsage software. The values in the brackets are results for P_{O_2}=0.21 atm.

Equilibrium phases	S1	S2	S3	S4
Slag-liquid	61.19 (54.27)	75.08 (61.86)	34.69 (32.36)	
$Ca_2MgSi_2O_7$_akermanite	15.81 (28.58)			
$CaSiO_3$_ps-wollastonite	15.96 (9.90)			
(MgO)(Cr_2O_3)_chromite	7.02 (7.26)	6.754 (7.13)	7.16 (7.28)	7.59 (7.52)
$Ca_3MgSi_2O_8$_merwinite		18.15 (31.01)	31.66 (47.21)	37.38 (40.16)
a-Ca_2SiO_4			26.48 (13.15)	54.89 (50.86)
Monoxide (CaO, MgO)				0.014 (1.46)

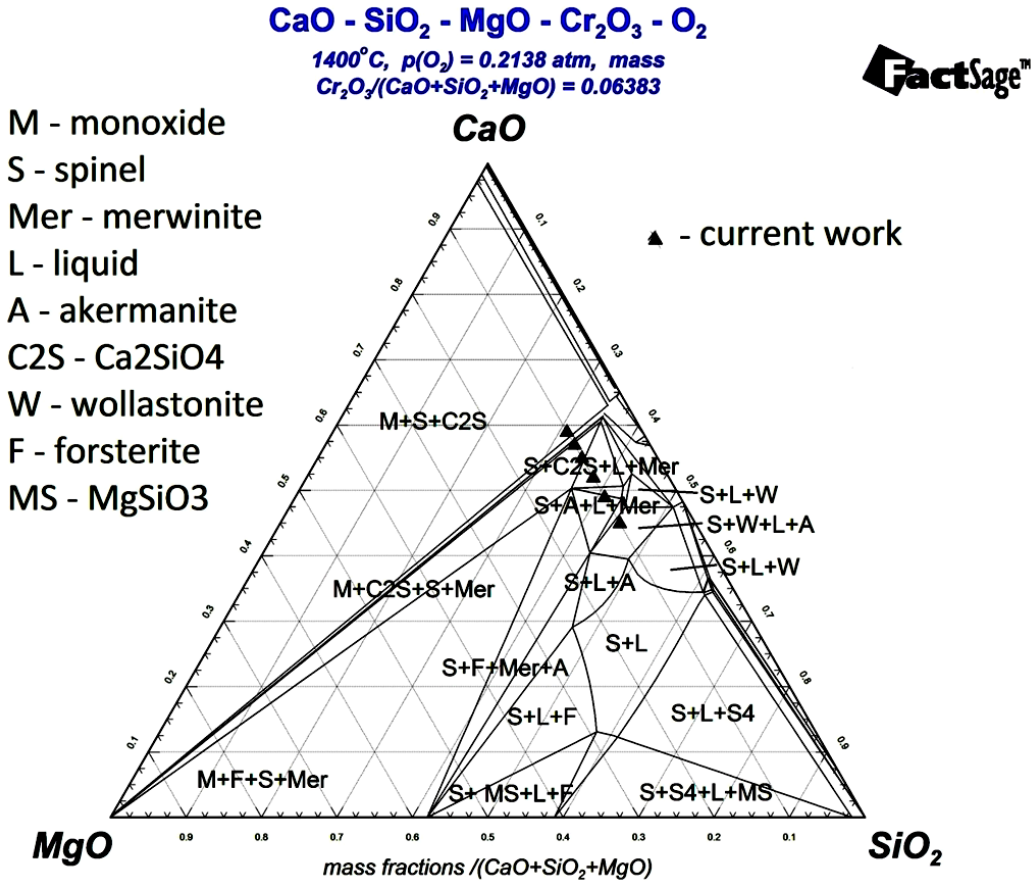

Figure 1 Isoterm for the CaO-MgO-SiO_2 -Cr_2O_3 system at 1673 K in air

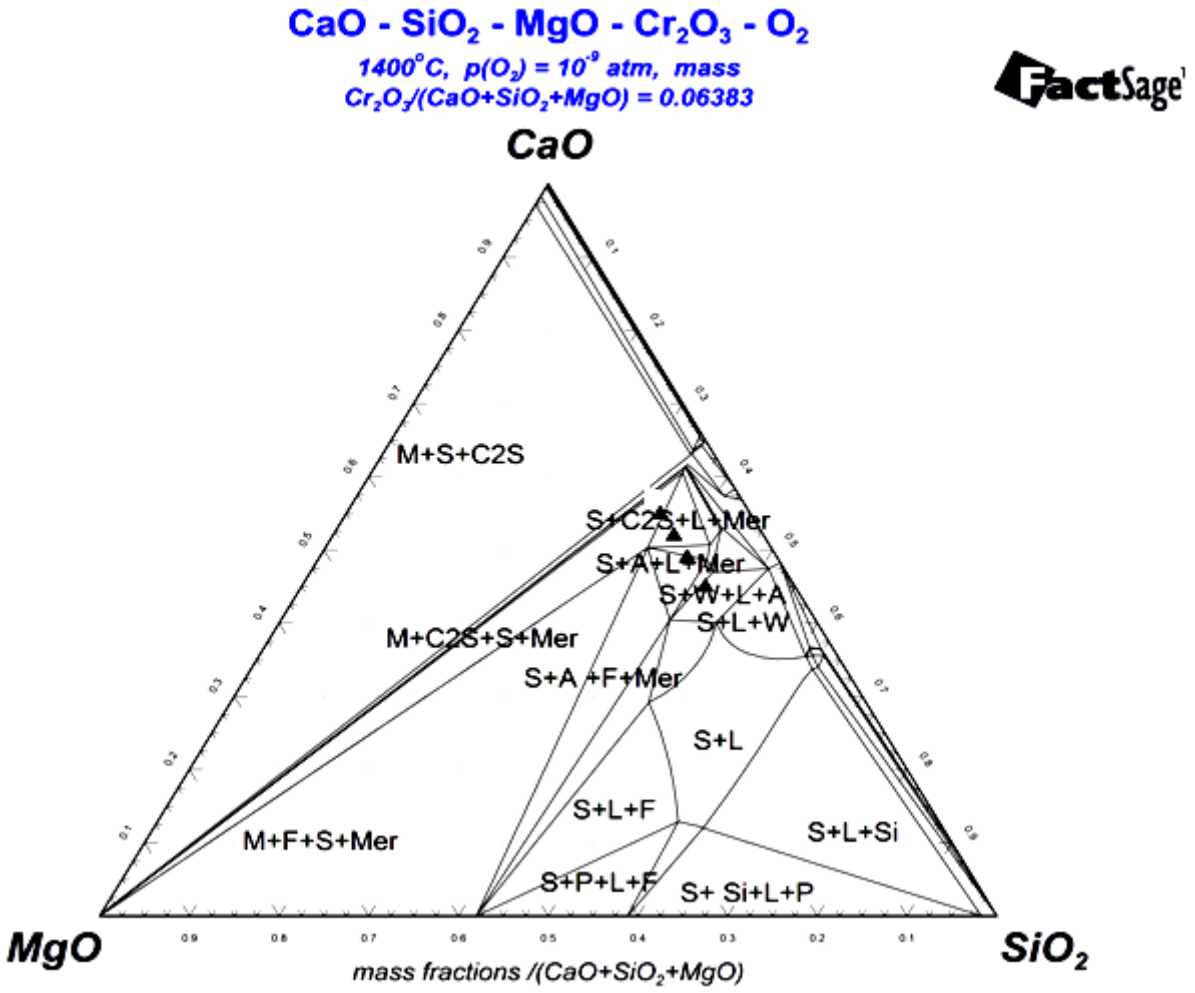

Figure 2 Isoterm for the CaO-MgO-SiO_2 -Cr_2O_3 system at 1673 K and oxygen partial pressure $P_{O_2}=10^{-4}$ Pa

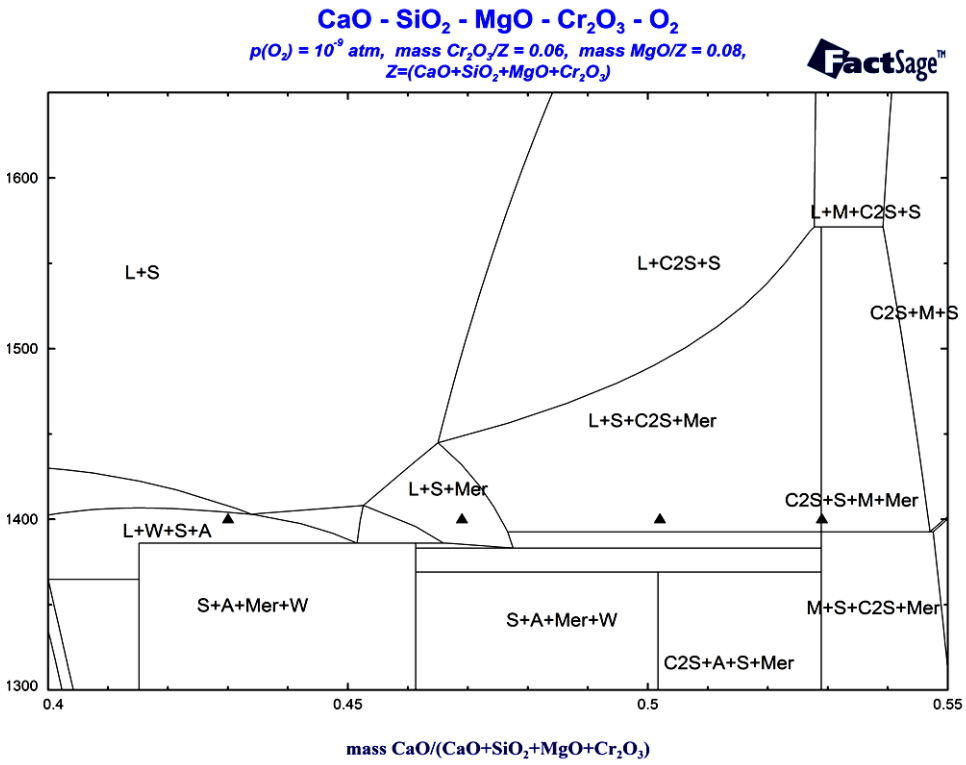

Figure 3 Isopleth for the CaO-MgO-SiO_2 -Cr_2O_3 system and oxygen partial pressure $P_{O_2}=10^{-4}$ Pa

2.2 Estimation of the chromium content in slag

The objective of the present investigation is to study chromium partition and phase relationships in the CaO-MgO-SiO_2-Cr_2O_3 slags with a view to control the precipitation of Cr-spinel and also to determine the activity of chromium oxide in the slag system. In the present work, the chromium containing slags kept in Pt crucibles were equilibrated with air and CO/CO_2 gas mixtures respectively, where the oxygen partial pressure was fixed to 10^{-4} Pa. The values of Cr activity in Pt are evaluated from the EDS analysis of the Pt –crucibles combining with a knowledge of the thermodynamics of the Pt-Cr system.

The equilibration reaction between the slag in the platinum crucible and the gas mixture can be represented as:

$$Cr(Pt)_{(s)} + \frac{x}{2}O_2 = CrOx(l) \qquad (1)$$

The values of Cr activity in Pt are evaluated from the EDS analysis of the Pt –crucibles.

The activity coefficient in Pt-Cr alloys according to Pretoris and Muan: [20] is given by the equation:

$$log_{10}\gamma_{Cr} = -4.42 - 11.39x_{Cr} - 7.35x_{Cr}^2 \quad (2)$$

Where γ_{Cr} and x_{Cr} are activity coefficient and mole fraction of Cr dissolved in Pt.

The ratio Cr^{2+}/Cr^{3+} were evaluated using following formula:

$$\log\left(\frac{x_{CrO}}{x_{CrO_{1.5}}}\right) = -\frac{11534}{T} - 0.25 \cdot \log(P_{O2}) - 0.203 \cdot \log(B) + 5.74 \quad (3)$$

Where T is temperature in K, P_{O2} is oxygen partial pressure in Pa and B refers to basicity defined as (wt%CaO+wt%MgO)/(wt%A_2O_3+wt%SiO_2) [17]

The ratio Cr^{2+}/Cr^{3+} was evaluated to be 0.005 for the samples in the range of basicities 1.0-1.6 soaked in air, which indicates that Cr_2O_3 is prevailing in the system. The value of x in CrO_x is 1.497. It can then be assumed that the following reaction is taking place:

$$2Cr_{(l)} + \frac{3}{2}O_{2(g)} = Cr_2O_{3(l)} \quad (4)$$

The standard Gibbs free energy for the reaction above was calculated using FACTsage software:

$$\Delta G_4^\circ = -701425[J] \quad (5)$$

The activity of Cr_2O_3 in the slag is then given by:

$$a_{(Cr_2O_3)} = \exp\left(\frac{-\Delta G_4^\circ}{RT}\right) \cdot a_{[Cr]}{}^2 \cdot (P_{O2})^{3/2} \quad (6)$$

Activity coefficients and activity values for samples SC1-SC4 soaked in air (basicity 1.0-1.6), evaluated from the Cr content based on EDS analyses of the Pt-crucibles are summarized in the table 2.

Table 2 Activity coefficients and activity values for samples SC1-SC4 soaked in air (basicity 1.0-1.6), evaluated from the Cr content based on EDS analyses of the Pt-crucibles.

Sample	Basicity	$x_{[Cr]Pt}$	$\gamma_{[Cr]Pt}$	$a_{[Cr]Pt}$	$a_{Cr2O3(slag)}$
SC1	1.0	1.06E-02	5.01E-05	5.31E-07	2.42E-03
SC2	1.2	1.25E-02	5.26E-05	6.58E-07	3.71E-03
SC3	1.4	1.34E-02	5.39E-05	7.22E-07	4.47E-03
SC4	1.6	1.13E-02	5.10E-05	5.77E-07	2.85E-03

The ratio Cr^{2+}/Cr^{3+} were also evaluated for the samples soaked at the oxygen partial pressure fixed to 10^{-4} Pa, values are summarized in the Table 3. The ratio Cr^{2+}/Cr^{3+} increases as a function of basicity .

The value of *x* in CrOx varies between 1.16-1.19, see table 3.

It can be assumed that two following reactions are taking place:

$$Cr_{(l)} + \frac{3}{4}O_2 = \frac{1}{2}Cr_2O_3(l) \qquad (4)$$

$$Cr_{(l)} + \frac{1}{2}O_2 = CrO(l) \qquad (7)$$

Gibbs free energy change for the reactions (4) and (7) were calculated using FACTsage software. Standard states chosen for Cr, CrO and Cr_2O_3 are pure liquids.

The activity of Cr_2O_3 in the slag is then given by:

$$a_{(CrOx)} = \exp\left(\frac{-\Delta G_1^{\circ}}{RT}\right) \cdot a_{[Cr]} \cdot (P_{O2})^{x/2} \qquad (8)$$

Where,

$$\Delta G_1^{\circ} = \mathrm{Xcro} \cdot \Delta G_2^{\circ} + \mathrm{Xcro}_{1.5} \cdot \Delta G_2^{\circ} \qquad (9)$$

Activity coefficients and activity values for samples S1-S4, the oxygen partial pressure was fixed to 10^{-4} Pa, (basicity 1.0-1.6), evaluated from the Cr content based on EDS analyses of the Pt-crucibles are summarized in the table 3.

Table 3 Activity coefficients and activity values for samples S1-S4, the oxygen partial pressure was fixed to 10^{-4} Pa, (basicity 1.0-1.6), evaluated from the Cr content based on EDS analyses of the Pt-crucibles.

Sample No.	Basicity (CaO/SiO_2)	($Xcro/Xcro_{1.5}$)	x value in CrOx	$x_{[Cr]Pt}$	$\gamma_{[Cr]Pt}$	$a_{[Cr]Pt}$	Xcro	$Xcro_{1.5}$	$aCro_x$
S1	1.0	0.677	1.161	1.20E-2	5.21E-5	6.25E-7	4.04E-1	5.96E-1	9.28E-3
S2	1.2	0.654	1.173	1.20E-2	5.21E-5	6.25E-7	3.95E-1	6.05E-1	8.82E-3
S3	1.4	0.635	1.182	1.20E-2	5.21E-5	6.25E-7	3.88E-1	6.12E-1	8.55E-3
S4	1.6	0.619	1.190	1.20E-2	5.21E-5	6.25E-7	3.82E-1	6.18E-1	8.31E-3

Chapter 3

Experimental Procedure

3. Experimental

3.1 Materials and sample preparation

Phase equilibrium studies of a set of synthetic $CaO-MgO-SiO_2-Cr_2O_3$ slags, each containing 6wt% Cr_2O_3 and 8wt% MgO, with basicities (CaO/SiO_2) in the range of 1.0 to 2.0 were conducted. The chemicals used and their purity grades are given in the Table 4. The slag compositions studied are presented in Table 5. CaO and MgO powders were calcined at 1273K (1000ºC) in a muffle furnace for 12h in order to decompose any hydroxide and carbonate. SiO_2 and Cr_2O_3 powders were heat-treated at 383K (110ºC) for 10 h in order to remove any moisture. After mixing the chemicals in appropriate proportions in an agate mortar, the powder mixtures were pressed into pellets of 15mm in diameter. The samples were placed in Pt crucibles, which were pressed out of platinum foil of thickness of 0.127mm and heat-treated at the required temperature in a gas mixture of CO/CO_2 gases to control the oxygen partial pressure. Oxygen partial pressure was kept at 10^{-4} Pa. (air of technical grade, supplied by AGA, Stockholm was used in the experiments in supplements I and II). The samples were preserved in desiccators to prevent re-absorption of water and CO_2 from atmosphere.

3.2 Gas cleaning system

In view of the low oxygen partial pressures targeted in the present study, as presented in supplement III, the gases used in the gas mixture were carefully purified before introducing into the reaction tube. The gas cleaning system consisted of a train of columns, present in the figure 4. Columns of silica gel, magnesium perchlorate and ascarite were used to remove the traces of H_2O and CO_2 from the commercial high purity grade gases. Columns of copper turnings were heated up to and kept at 823K, to remove the residual O_2. The gases were mixed in a chamber filled with glass beads, before introducing the mixture into the reaction tube. The gas ratios used in the present study were pre-calculated using FACTsage software in order to meet the required oxygen partial pressure. Bronkhorst High-Tech Flow-bus E600 mass flow meters were used to control the flow rates of the involved gases. A narrow gas inlet tube (5mm inner diameter) led the gas mixture directly into reaction zone just above the slag samples in order to minimize the error due to thermal segregarion of the gases in the gas mixture.

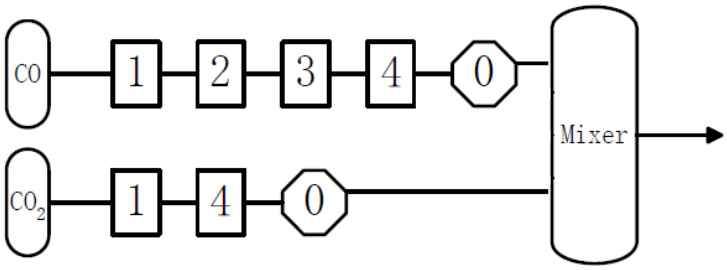

Figure 4 Schematic illustration of gas cleaning system: 0 – flowmeter; 1- silica gel; 2- magnesium percholorate; 3- ascarite; 4- copper turnings. Adopted from [17].

Table 4 Purity of the chemicals used

Chemical	Purity	Supplier
Pt-foil	99.99%	Alfa-Aesar, Germany
Cr_2O_3	98%	Sigma-Aldrich
SiO_2	98%(Reagent grade)	Sigma-Aldrich
MgO	98%	Sigma-Aldrich
CaO	98%	Sigma-Aldrich

Table 5 Chemical composition of the original slag samples

Sample No.	Composition (wt%)				
	Basicity	CaO	SiO_2	MgO	Cr_2O_3
S1	1.0	43.0	43.0	8.0	6.0
S2	1.2	46.9	39.1	8.0	6.0
S3	1.4	50.2	35.8	8.0	6.0
S4	1.6	52.9	33.1	8.0	6.0

3.3 Principle of the experimental method

Classical gas/slag equilibrium technique was adopted in this work. The samples with targeted compositions were kept in Pt crucibles and were equilibrated with air as well as a gas mixture of CO/CO_2 gases to control the oxygen partial pressure. In the later case, the oxygen partial pressure was kept at 10^{-4} Pa at the required temperature. The samples were then quenched directly or slow cooled to1673 K and soaked at that temperature for 24h. The cooling rate was 2K/min.

3.4 Apparatus

Figure 5 shows the schematic arrangement of the furnace reaction tube. The furnace was equipped with $MoSi_2$ heating elements. The furnace was controlled by a Eurotherm PID controller equipped with PtRh30%/PtRh6% thermocouple as the sensor. The temperature deviation at the even temperature zone of the furnace that extended to about 80 mm at the centre of the reaction tube was found to be less than ±3K.

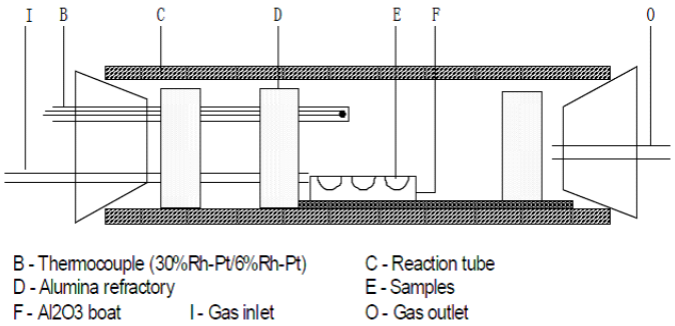

Figure 5 Schematic arrangement of the furnace reaction tube [17]

3.5 Procedure

The Pt crucibles containing the samples were positioned inside an alumina holder. Before the heating of the furnace, the alumina sample holder was pushed into the furnace and positioned in the even-temperature zone. The furnace was heated at a heating rate of 5K/min with eather air or a gas mixture of CO/CO_2 flowing through the reaction tube. The gas flow rate was 100ml/min. After the targeted temperature was reached, the samples were equilibrated for 24h in air or a gas mixture of CO/CO_2 gases to control the oxygen partial pressure. In the later case the oxygen partial pressure was kept at 10^{-4} Pa.The samples were then slow cooled at a cooling rate of 2K/min to 1400C and soaked for 24h at very low P_{O2}. The samples were quenched by pulling them quickly to the water-cooled cold end of the reaction tube and then dropped into distilled water kept at room temperature. The samples were carefully dried and kept in desiccator. The quenched samples were analyzed using SEM, EDS and XRD

techniques. For the XRD analysis SIEMENS D5000 X-Ray Diffractometer (K_α–Cu) was used. SEM analyses were carried out using a Hitachi S3700N SEM unit equipped with Bruker SDD–detector for EDS analysis. Selected experiments were repeated and the results were found to be reproducible.

Chapter 4

Results and Discussion

4.1 Effect of the basicity and the heat treatment on the chromium partition

Figure 6 is the SEM micrograph of the sample S1 with basicity 1.0 after a heat treatment at 1873 K (1600 ºC) for 24h. Sample is mainly consisted of liquid slag quenched from 1873 K (1600 ºC). XRD analysis comfirmed that the sample is mainly amorphous. In addition to the amorphous silicate matrix, spinel crystals were found in the sample. The grain size of the spinel phase is max. 20 µm. The phases present and phase compositions in the sample S1 are given in Table 6.

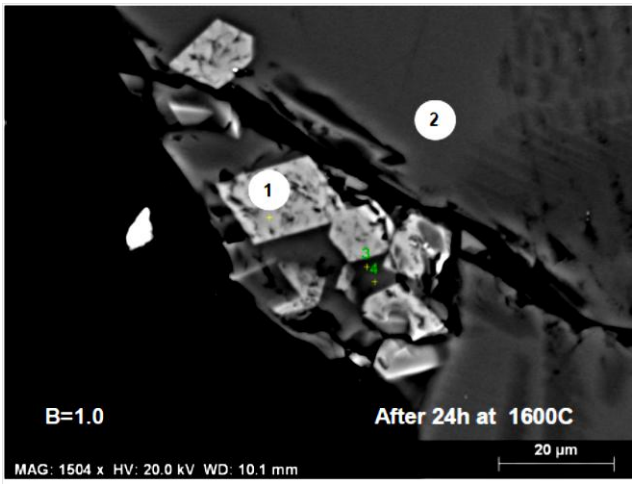

Figure 6 SEM picture of the sample S1 with basicity 1.0 after a heat treatment at 1873 K (1600 ºC) for 24h and quenched. Phase (1) corresponds to Spinel crystals (grain size max. 20 µm). Phase (2) is matrix amorphous.

Table 6 EDS analysis at% of the slag sample S1

	Ca	Mg	Si	Cr	O*
(1) spinel	0.80	12.83	0.03	28.74	57.60
(2) matrix	22.06	4.80	16.44	1.10	55.60

*Oxygen contents are considered unreliable

Figure 7 shows SEM micrograph of the sample S2 with basicity of 1.2. A considerable amount of spinel phase was found in the sample with 10 – 20 µm in diameter. EDS spectra of the sample show that the matrix consists of chromium-containing calcium magnesium silicates $(Ca,Mg)(Si,Cr)O_x$. The composition variations in the sample are given in the Table 7.The phases present according to XRD are merwinite, spinel and wollastonite. From the XRD curve of the sample, it can also be concluded that some parts of the sample remain amorphous. The presence of spinel phase was also confirmed by XRD analysis. The matrix consists of merwinite dendrites surrounded by liquid phase with some amount of wollastonite.

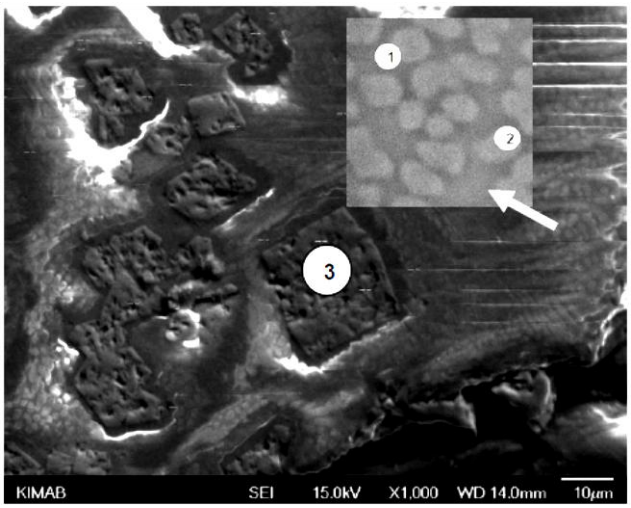

Figure 7 SEM micrograph of the sample S2 with basicity 1.2 quenched after 24h at 1873 K(1600 ºC) .

(1) amorphous matrix; (2) merwinite; (3) spinel phase 10 – 20 µm in diameter.

Table 7 EDS analysis at% of the slag sample S2

	Ca	Mg	Si	Cr	O
(1) matrix	20.91	5.39	12.26	1.40	60.03
(2) merwenite	19.89	3.53	14.48	1.69	60.40
(3) spinel	0.92	12.64	0.54	22.54	63.30

Figure 8 shows slag sample S3 with basicity 1.4 after heat treatment at 1873 K (1600 ºC) for 24h. Fine (2.5 µm) polygonal spinel crystals (1), merwinite lamella (2) and eutectic, mostly consisting of wollastonite and Cr –rich particles (3) can be observed. The composition variations in the sample are given in the Table 8.

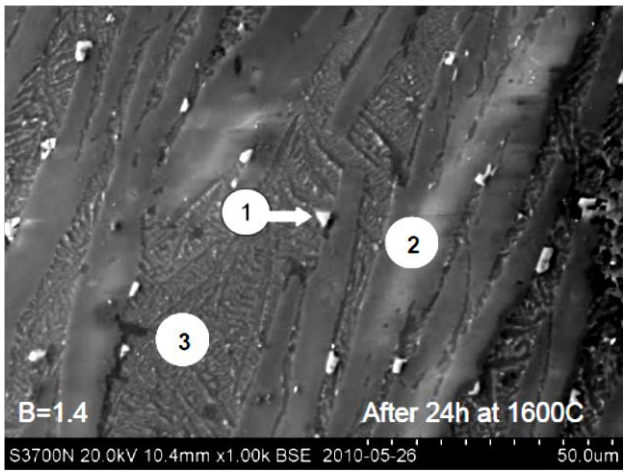

Figure 8. Slag sample S3 with basicity 1.4 quenched after heat treatment at 1873 K (1600 ºC) for 24h.

(1): Fine (2.5 µm) polygonal spinel crystals; (2): merwinite lamella; (3): eutectic, mostly consisting of wollastonite and Cr –rich particles.

Table 8 EDS analysis at% of the slag sample S3

	Ca	Mg	Si	Cr	O
(1) spinel	2.17	13.31	2.17	32.27	50.07
(2) merwinite	27.32	8.67	18.94	0.69	44.37
(3) eutectic	24.25	0.75	23.74	1.05	50.19

Figure 9 shows chromium-rich dendrites and well-developed spinel crystals in the sample S4. The dendrite structure consisted of spinel solid solution and had a chromium content of 8.32at% and 63at% oxygen. However, it is admitted that the EDS oxygen analyses are uncertain. The spinel phase $(Ca,Mg)Cr_2O_4$ with some impurities of Si and Ca, had chromium and oxygen content of 14.90 and 67.32 mole percent respectively. The matrix phase exhibited a concentration variation where areas close to spinel precipitates had less Cr (1.6at %) compared to the chromium content in-between the spinel crystals which was slightly higher, approximately 5.2at%. The overall Cr content in the matrix was found to be high and close to the original (6wt%). Magnesium content in the matrix varied between 2 to 6 mole percent. Oxygen concentration in the matrix phase was around 57 mole percent and in the spinel phase around 68. Complete compositions of the phases obtained are given in the Table 9.

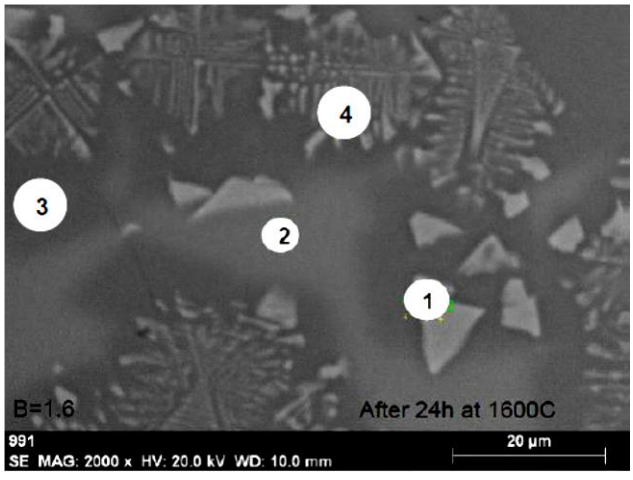

Figure 9. Slag sample S4 with basicity 1.6 quenched after heat treatment at 1873 K (1600 ºC) for 24h.

(1): Fine (<10µm) polygonal spinel crystals; (2) and (3): calcium magnesium silicate matrix; (4): chromium rich dendrites.

Table 9 EDS analysis at% of the slag sample S4

	Ca	Mg	Si	Cr	O
(1) spinel	6.78	7.59	3.40	14.90	67.32
(2) matrix	21.91	2.28	10.28	5.17	60.36
(3) matrix	22.44	6.12	11.66	1.61	58.16
(4) dendrite	13.91	6.75	7.09	8.32	63.93

Figure 10 shows XRD graphs for the samples S1-S6 after heat treatment at 1873 K (1600 ºC). The phases frequently found in the samples are merwinite, wollastonite and calcium silicate Ca_2SiO_4. In the sample S2 with basicity of 1.2, the phases present according to XRD are merwinite, spinel and wollastonite. From the XRD pattern, it can be concluded that the sample S1 is mostly amorphous, as can be seen in Figure 10. In the sample S3, merwinite $Ca_3Mg(SiO_4)_2$, wollastonite and calcium silicate Ca_2SiO_4 were found as can be seen in the XRD pattern (Figure 10). SEM analysis confirms that considerable amount of spinel phase as well as merwenite lamella are formed. The sample S4 consists of wollastonite, merwinite and Ca_2SiO_4 phases. In the sample S5, the matrix consists of a solid solution of calcium silicates Ca_2SiO_4 phases, as well as periclase, and merwinite. Peaks for β - Ca_2SiO_4 and γ- Ca_2SiO_4 are marked by *b* and *g* respectively. Periclase particles found in the sample S5 were up to 50μm in size. In the case of sample S6 with basicity 2.0, (Figure 10), both Ca_2SiO_4 phases and merwenite containining periclase (MgO) were observed. The MgO content in the slag was however relatively low, which makes the intensity of XRD quite small.

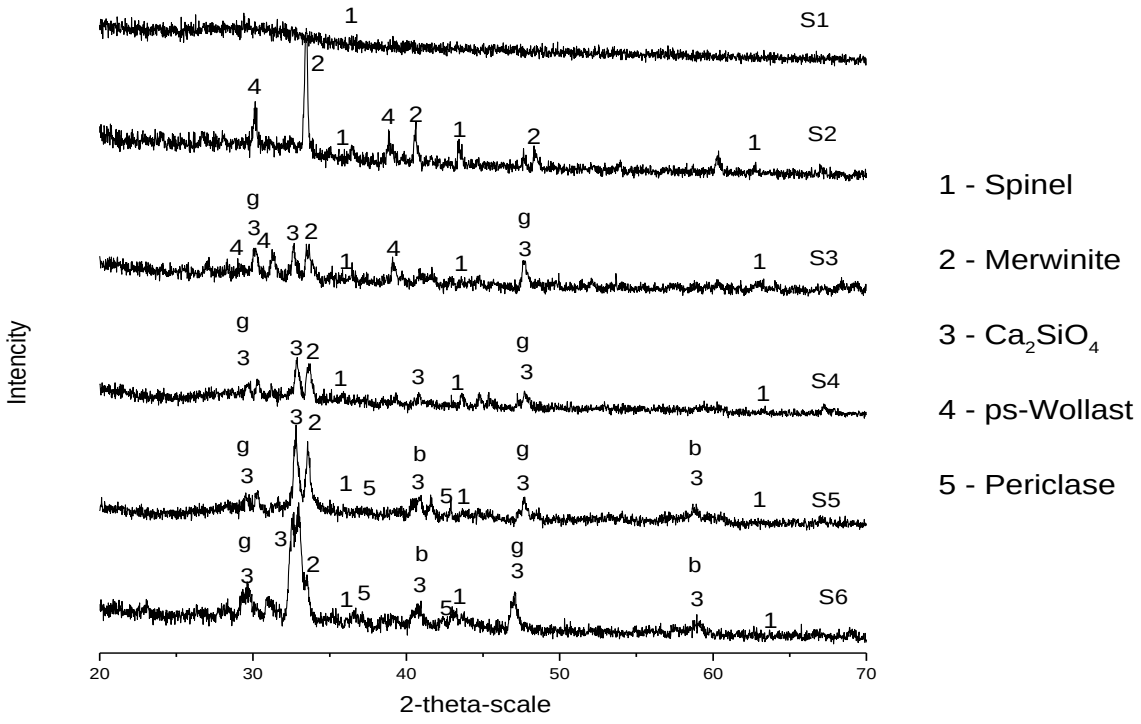

Figure 10 XRD pattern for the samples S1-S6 heat treated at 1873 K, the 2-θ values are in the range of 20 to 70°

From the XRD pattern for the sample S1 and, it can be concluded that the matrix is highly amorphous. It was found that the sample S1 consisted of liquid slag before quenching from 1873 K (1600 ºC). SEM analysis showed that the samples S1 and S2 (basicities 1.0 and 1.2) contained, in addition, precipitated spinel crystals 10 – 20 µm in diameter.

Pseudo-wollastonite was found in the sample S2 and S3. According to the literature [17], pseudo-wollastonite should appear in the quenched slag rather than wollastonite[17, 18]. Wollastonite has triclinic crystals although pseudo-wollastonite has monoclinic crystal structure. Besides the crystal structure, their melting temperatures differ considerably. The melting temperature of wollastonite and pseudo-wollastonite are 1523K (1250ºC) and 1785K (1512ºC) respectively. The transition temperature of wollastonite into pseudo-wollastonite is 1453K. Pseudo-wollastonite is likely to have been formed on quenching. Merwinite phase

was found in samples S2-S5. This phase is also considered to be unstable at 1873 K [19], but were confirmed by XRD and SEM.

Figure 11 shows isopleth in the CaO-MgO-SiO_2 -Cr_2O_3 system in air atmosphere, where Cr_2O_3 and MgO are fixed to 6wt% and 8% respectively and oxygen partial pressure to 0.21 atm. There is clear disagreement between experimental results and thermodynamic calculations by FACTsage regarding merwinite phase. There should be no merwinite phase in the sample S2 and S3 according to the calculated diagram presented in Figure 11. However, merwinite phase was found in our experimental samples S2 and S3. More experiments are required in order to determine the stability region of merwinite. Pseudo-wollastonite was also found in the samples with low basicities. Even here further investigations of the stability region could be needed.

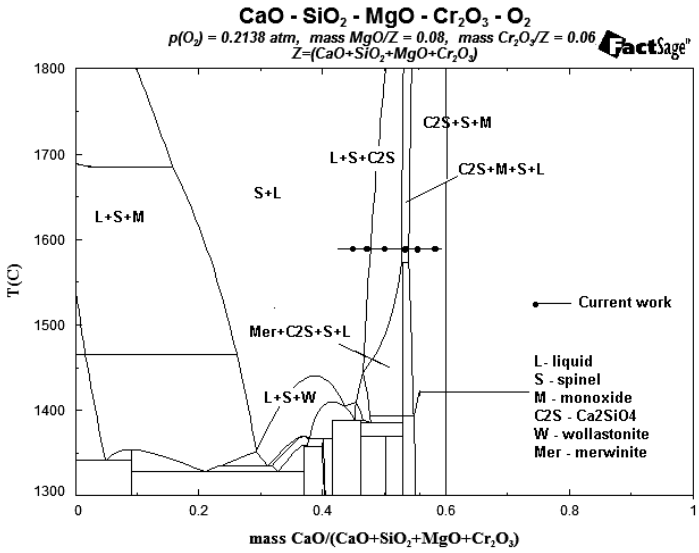

Figure 11 Isopleth in the CaO-MgO-SiO_2 -Cr_2O_3 system at in air atmosphere, where Cr_2O_3 and MgO are fixed to 6wt% and 8% respectively and oxygen partial pressure to 0.21 atm.

According to SEM, the spinel phase was present in the samples S1-S4. In samples S3 and S4, the matrix consists of a mixture of silicate, and merwinite and the average Cr content is a maximum of 5at% of dissolved chromium, the oxygen content being about 57at%. In the matrix close to the spinel surface, the chromium content is found to be 1.6at%, showing that the spinel growth occurred from the matrix. The chromium rich dendrites (spinel solid

solution) were formed in the samples S4 and S5. The Cr content in the matrix in the samples S4-S6 is high and close to the start composition of the reagent mixture.

It can be concluded that the samples S1, S2, S3 and S4 were quenched from liquid state and samples S5 and S6 from solid state (remain unmelted). β - Ca_2SiO_4 and γ- Ca_2SiO_4 found in the samples, according to XRD are not stable at 1873 K (1600 ºC) and have been transformed from α-Ca_2SiO_4 at lower temperatures. Ca_2SiO_4 can exist in five polymorphic phases, among which only two are stable at room temperature. The β - Ca_2SiO_4 phase, forms usually in the presence of impurity ions and easily reacts with water. The foreign ions, Cr as in this work would leach out if exposed to the water. One other stable polymorphic phase is γ- Ca_2SiO_4 which does not react with water [1, 20], but disintegrates to dust.

SEM and EDS techniques confirmed the FACTsage calculations, that spinel phase can be successfully precipitated at 1873K (1600 ºC) in air atmosphere at slag basicities in the rage of 1.0 - 1.6. The reason for this could be that, within this composition range, the slag is still in the liquid state, close to the liquidus temperatures, giving larger driving force for the precipitation of the crystals, but still holding a fast diffusion of the ions. Spinel formation is a kinetically control phenomenon. At higher basicities, the samples are in the solid state during the entire procedure hindering the movement of ions, thus requiring longer time to reach thermodynamic equilibrium.

The magnesiochromite spinel phase ($MgCr_2O_4$) found in the samples contained some impurities of CaO and SiO2, according to EDS analysis. However the results could be affected by the surrounding matrix if the electron beam was in contact with it.

There is a certain risk for formation of solid solution of Cr with phases periclase and merwinite, as well as the formation of $CaCr_2O_4$ at higher basicities, that could lead to Cr leaching. Thus, basicities higher than 1.4 have to be avoided since there is a risk of formation of Cr-rich solid solutions that might leach out.

Figure 12 shows XRD curves for the samples SC1-SC6 with basicities in the range 1.0-2.0. Phases present are spinel, ps-wollastonite, merwinite, Ca_2SiO4, rankinite, periclase, Cr-oxide and $Ca_7Mg(SiO_4)_4$. The strong peak of the curve corresponding sample SC1 matches with Mg-chromite spinel phase. $Ca_7Mg(SiO_4)_4$ was found in the samples SC2-SC6 which is not in agreement with FACTsage calculations, see table 1.

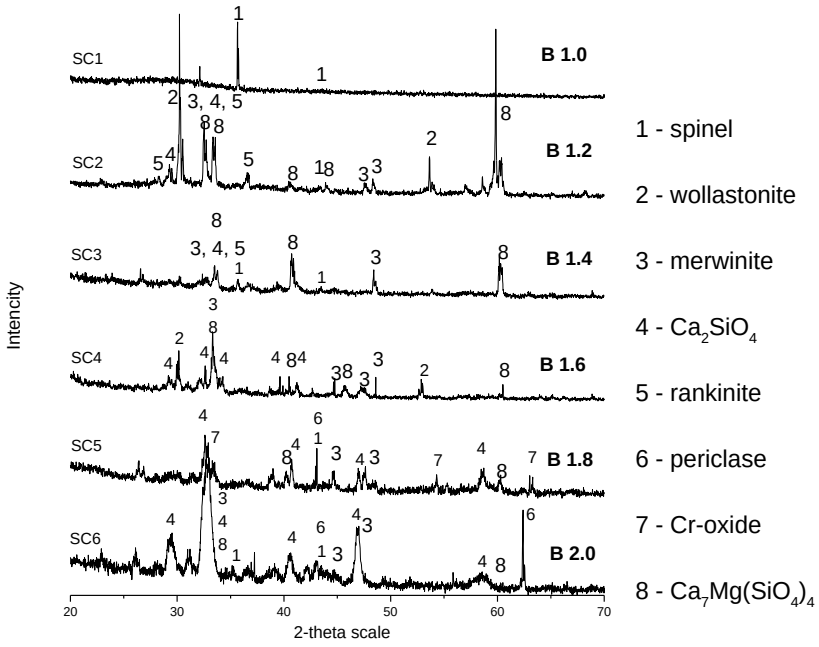

Figure 12 XRD curves for the samples SC1-SC6 with basicities in the range 1.0-2.0.

Figure 13 shows the SEM image of the sample SC1 with basicity 1.0. The sample was first equilibrated in air at 1873 K for 24h, then slow cooled and soaked at 1673 K for additional 24h. It was observed that the sample remains liquid down to 1673 K. The matrix was found to be amorphous. The Cr content in the matrix was observed to be low and was evenly

distributed. The chromium content in the matrix was lower compared to the samples that have been directly quenched after equilibration at 1873 K. The amount of impurities in the spinel phase (Ca, Si) had also decreased compared to directly quenched sample. Phases present and the EDS analysis of the sample SC1 are amorphous matrix and spinel phases, see table 10. The grain size of the spinel increased by one order of magnitude (max. 200 µm) as compared with the sample which was directly quenched after quenched from 1873 K. In the Pt – crucible: chromium content according to EDS analysis is 1.06 at%. Cr is evenly distributed throughout the Pt-crucible cross section, which indicates that the system was close to equilibrium.

The present observations indicate that the sample is highly amorphous and contains some amount of the spinel phase. There is certain disagreement between the experimental results and FACTsage calculations. None of the phases, akermanite $Ca_2MgSi_2O_7$, or ps-wollastonite $CaSiO_3$ were detected by XRD or SEM in the sample SC1. The strong peak of the XRD curve corresponding to sample SC1 matches with Mg-chromite spinel phase. From the shape of the XRD curve of the sample SC1, it can be concluded that the sample was mainly amorphous. Phases stable according to FACTsage calculation are slag-liquid, $Ca_2MgSi_2O_7$ akermanite $CaSiO_3$ ps-wollastonite and $(MgO)(Cr_2O_3)$ chromite spinel phase , see table 1.

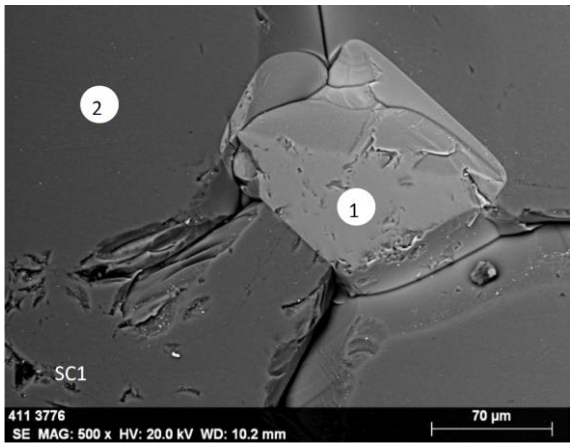

Figure 13. Sample SC1 with basicity 1.0. The grain size of the spinel increased by one order of magnitude (max. 200 µm) compared with the sample being directly quenched from 1873 K.

Table 10 EDS analysis of the sample SC1 (mole%)

	Cr	Ca	Si	Mg	O
(1) spinel	32.30	0.37	0.08	13.22	54.03
(2) matrix	0.74	21.79	17.38	4.96	55.13

Figure 14 shows SEM micrograph of the sample SC2 with basicity 1.2 slow-cooled to and soaked at 1673 K, a) large spinel grains, up to 200µm in diameter, can be observed, b) shows the matrix at higher magnification. The matrix consisted of merwenite dendrites and the ps-wollastonite matrix. The spinel grain size increased more than one order of magnitude after slow cooling and soaking at 1673 K. The Cr content in the merwinite dendrites slightly decreased after slow cooling. Phases present and the EDS analysis of the sample SC2 are given in the Table 11. The Cr content in the Pt- crucible is found to be 1.25 at% according to EDS analysis.

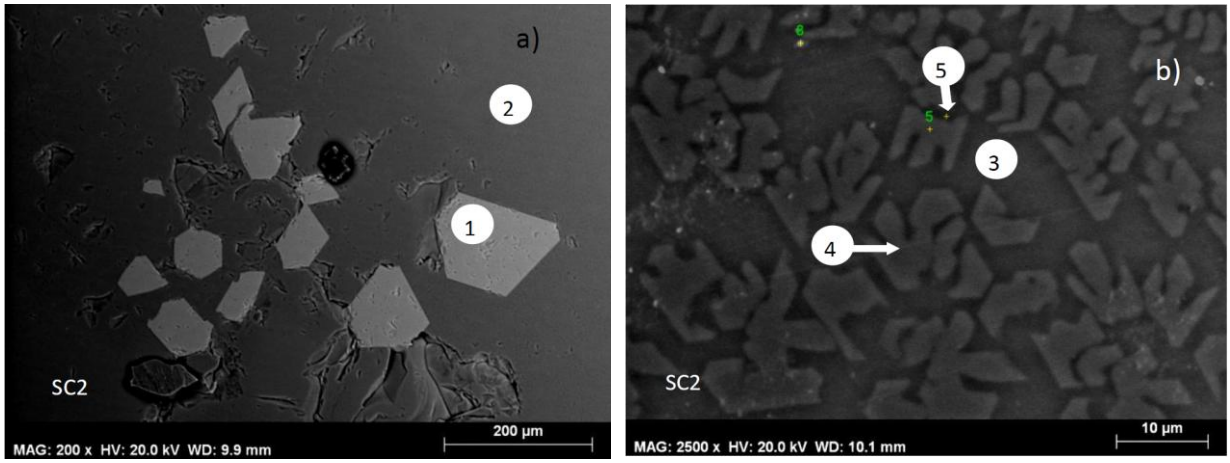

Figure 14. SEM micrograph of the sample SC2 with basicity 1.2 slow-cooled to and soaked at 1673 K, a) Overview of the microstructure: (1) large up to 200 µm in diameter spinel grains can be observed, (2) matrix, b) matrix at higher magnification: The matrix consisted of (3) ps-wollastonite matrix and (4) merwinite dendrites, (5) rankinite $Ca_3Si_2O_7$ phases.

Table 11 EDS analysis of the sample SC2(mole%)

	Si	Cr	Ca	Mg	O
(1) spinel	0.25	37.80	0.55	14.72	46.69
(2) matrix	15.95	0.82	28.71	6.58	47.94
(3) ps- wollastonite	18.90	1.47	26.75	3.49	49.39
(4) merwinite	15.53	0.90	29.14	6.74	47.70
(5) matrix	21.18	1.44	26.80	5.44	45.14
(5) rankinite $Ca_3Si_2O_7$	16.90	1.46	25.80	3.47	52.38

Phases thermodynamically stable at this temperature and composition according to FACTsage calculations are slag liquid, merwinite $Ca_3MgSi_2O_8$, and magnesium chromite $(MgO)(Cr_2O_3)$ spinel phase. Figure 12 shows XRD graph for the samples with basicity 1.2, where the phases spinel and merwinite are confirmed. From SEM pictures as well as the shape or XRD curve for sample SC2, it can also be concluded that the matrix was amorphous to some part. In addition, Ca_2SiO_4, $Ca_7Mg(SiO_4)_4$, ps-wollastonite and rankinite were found according to XRD, which is in disagreement with calculated results.

Figure 15 a), b) shows sample SC3 with basicity 1.4. The phases present are Ca_2SiO_4, merwinite, spinel; and possibly $Ca_7Mg(SiO_4)_4$. From the Figure 15 a), it can be concluded that some amount of the spinel solid solution phase has precipitated and grown from Ca_2SiO_4 phase on cooling. The Pt-crucible contained 1.34 at% Cr according to EDS. Figure 12 shows XRD patterns for the sample SC3 with basicity 1.4. The sample contained phases spinel, wollastonite, merwinite, Ca_2SiO_4, Cr-oxide, and $Ca_7Mg(SiO_4)_4$. The main part of the sample was however amorphous. Phases thermodynamically stable at this temperature and composition (sample SC3 basicity 1.4) according to FACTsage calculations are slag liquid, merwinite $Ca_3MgSi_2O_8$, spinel, and a-Ca_2SiO_4 (see table 1).

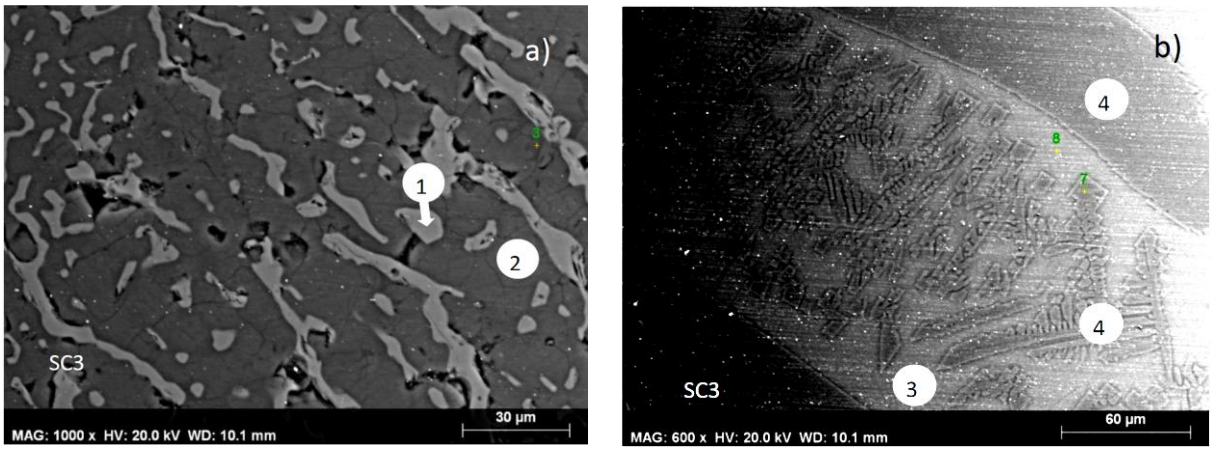

Figure 15. Sample SC3 basicity 1.4.

a) (1) spinel solid solution; (2) Ca_2SiO_4,

b) (3) matrix, (4) merwinite,

Table 12 EDS analysis of the sample SC3(mole%)

	Cr	Ca	Si	Mg	O
(1) spinel	30.27	1.53	0.20	13.15	54.85
(2) Ca_2SiO_4	0.87	33.17	14.055	1.525	50.38
(3) matrix	1.61	25.53	16.91	2.42	53.55
(4) merwinite	0.54	27.42	14.12	7.23	50.69

Figure 16 shows sample SC4 with basicity 1.6. Phases present are spinel solid solution, Ca_2SiO_4 and $Ca_3MgSi_2O_8$ merwinite. Phases present according to FACTsage for the sample SC4 (B=1.6) are: spinel, merwinite, a-Ca_2SiO_4 and monoxide solid solution (consisting of CaO, MgO) (see table 1). XRD analysis for the sample SC4 (basicity 1.6), (see Figure 12), confirmed the presence of spinel, merwinite and Ca_2SiO_4. Phases ps-wollastonite and $Ca_7Mg(SiO_4)_4$ were also found. Small amounts of phases periclase, Cr-oxide and $CaMgSi_2O_6$ were also detected according to XRD. Spinel phase precipitated at earlier stage had a regular spinel shape and had less impurities (CaO). The spinel solid solution $Mg(Ca,Cr)O_4$ precipitated from Ca_2SiO_4 on cooling had a significant amount of Ca and Si impurities.

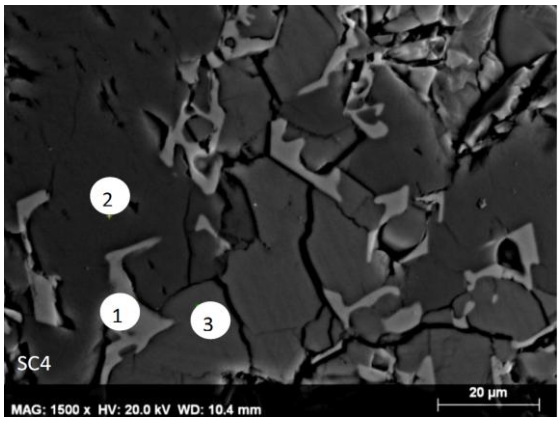

Figure 16. Sample SC4 with basicity 1.6 phases present: (1) spinel solid solution, (2) merwinite, (3) Ca_2SiO_4

Table 13 EDS analysis of the sample SC4(mole%)

	Cr	Ca	Si	Mg	O
(1) spinel	27.51	1.98	0.70	13.21	56.60
(2) merwinite	0.52	27.37	13.73	7.41	50.99
(3) Ca_2SiO_4	0.76	32.25	13.78	2.53	50.68

The EDS analysis of the chromium dissolved in Pt crucible for samples with basicity 1.6 and higher slightly varied as a function of distance. Furthermore, samples with basicities higher than 1.4 were found incompletely melted or not melted at all. This is interpreted by the present authors that equilibrium was not reached.

Figure 17 a) shows Cr partition in CaO-MgO-SiO_2-Cr_2O_3 slag system at 1673K and 1873K respectively. The equilibration experiments were conducted in air atmosphere. In general, chromium content in the calcium silicates matrix decreased after slow cooling to 1673K compared to the samples that been quenched from 1873K, see fig 12a). In both cases the chromium partition in the system is a function of basicity. It was found that the amount of impurities (CaO and SiO_2) in the spinel phase increases with increased basicity. The slight decrease of the chromium content in the matrix is due to accumulation of the Cr in the periclase phase found in the samples at the basicities higher than 1.6.

Variation in Cr content in spinel and matrix phases respectively are plotted as a function of basicity (CaO/SiO_2). The peak at a basicity 1.4 in the upper curve shows that the spinel phase precipitated did not dissolved foreign elements, and that the driving force for its formation was rather high. The dip of the Cr_2O_3 content in the spinel phase at basicity 1.2 could be within the experimental scatter. At the higher basicities, spinel is found to dissolve CaO. It is

interesting to note that the sharp decrease in the upper curve matches with the slight increase in the bottom curve. The latter will show only a small increase as the amount is much higher. As the basicity increases the Cr gets dissolved in other phases, for example the Cr content in periclase is extremely high. Chromate clusters may be expected to be formed together with Ca ions in the liquid slags tending to precipitate out the chromate phase at lower temperatures. This may be plausible explanation of the Cr partition trend.

Figure 17 b) shows the activity of liquid Cr_2O_3 in CaO-MgO-SiO_2-Cr_2O_3 slag system at 1673 K as a function of basicity. The plot shows a sharp decrease between basicity 1.4 and 1.6. This would mean that the chemical potential of Cr_2O_3 is decreased in the slag and thus, Cr_2O_3 will attempt to accumulate in the slag matrix phase. Since the amount of the slag matrix phase is significant compared to the spinel phase, the increase in the amount of Cr_2O_3 in the silicate matrix phase will not be reflected in the EDS analysis. On the other hand, the decrease in the spinel phase is noticeable and can be seen to follow the same pattern. Decrease in the activity of Cr_2O_3 in the slag matrix phase would correspond to the decrease in the amount of Cr_2O_3 in the spinel phase. The effect is very clear at lower temperatures. When the temperature is increased, the entropy factor dominates. Thus, the system tends towards ideality and the effect of the reduced chemical potential may not be apparent. The decrease in the activity of Cr_2O_3 in the slag at basicities 1.4 to 1.6 is likely to be due to the formation of spinel species in the slag, assuming that the slag is homogeneous, leading ultimately to its precipitation.

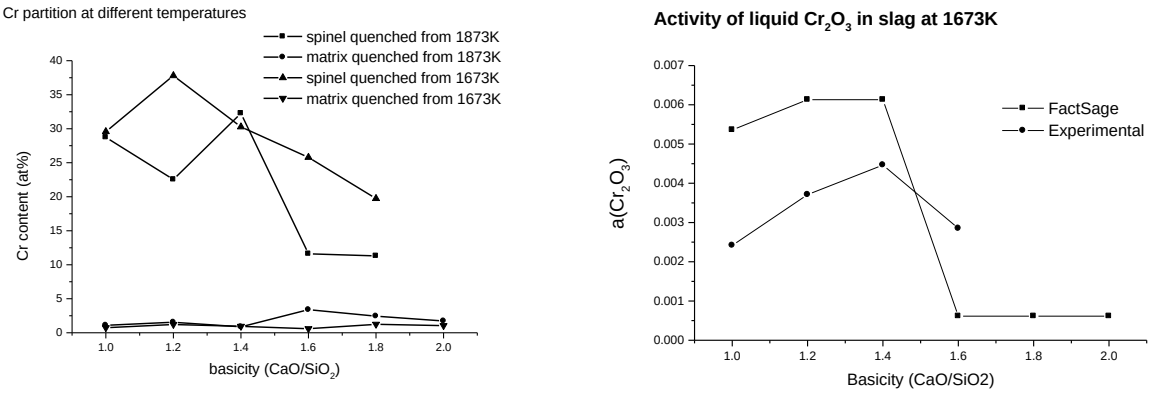

a) b)

Figure 17 The equilibration experiments were conducted in air atmosphere. a) Cr partition in CaO-MgO-SiO_2-Cr_2O_3 slag system at 1673K and 1873K respectively. b) Activity variation of liquid Cr_2O_3 in CaO-MgO-SiO_2-Cr_2O_3 slag system at 1673K as a function of basicity. The results of thermodynamic calculation by FACTsage software are summarized and compared with the experimental results from the current work.

The Cr content in the matrix slightly decreased after slow cooling as result of spinel growth. The Cr content in the merwinite dendrites for the sample SC2, basicity 1.2 slightly decreased after slow cooling due to lower solubility of foreign elements at lower temperature. The

merwinite phase rejected dissolved chromium oxide into matrix as the temperature decreased. As a result the Cr rejected by merwinite phase was precipapted to form spinel phase in the matrix.
There is potential for further spinel growth, since both MgO and Cr-oxide are present in the matrix, see table 5. Glass formation is possible if the sample is quenched rapidly. Glass phase is also stable toward dissolution and thus will hinder Cr leaching. Phases present and the EDS analysis of the sample SC2 are given in the Table 5. The Cr content in the Pt- crucible is found to be 1.25 at% according to EDS analysis. Ps-wollastonite could be formed on quenching from liquid slag in the samples with basicity 1.2 -1.4

In the sample SC3 basicity 1.4, $Ca_7Mg(SiO_4)_4$ phase was not predicted by FACTsage.

According to XRD analysis, see figure 12, the presence of free Cr-oxide, at higher basicities is probably due to the fact that MgO was bound into merwinite and $Ca_7Mg(SiO_4)_4$ phases and thus could not form spinel.

The spinel grain size has increased by one order of magnitude in the samples SC1 and SC2 after slow cooling and soaking at 1673K compared to the samples that have been directly quenched after equilibration at 1873K. The impurity content in the spinel phase is decreased after slow cooling in all samples. The amount of the CaO dissolved in the spinel phase is found to increase as a function of basisity. As a result of efficient spinel phase growth, the chromium content is decreased in the matrix. The chromium content in the merwinite and Ca_2SiO_4 phases decreased after slow cooling. Some amount of the spinel phase has precipitated and grown from Ca_2SiO_4 phase on cooling as can be seen in the case of samples SC4. Chromium dissolved in matrix phases at higher temperatures was precipitated as spinel as the temperature decreased due to low solubility of Cr in the matrix phases at lower temperature. Crystallization is a process where the atoms are transferred from the disordered liquid state to the more ordered solid state. The rate of the crystallization process or crystal growth is described and controlled by kinetic laws. Driving force of solidification is proportional to supercooling or supersaturation. With increased concentration, there is a tendency of the atoms to be incorporated into the crystal. There is also a tendency of the atoms surrounding the crystal to get adsorbed at the interface to cluster together [19]. The diffusion of atoms or ions in the melt is high compared to solid state and the driving force of spinel formation is high due to cooling. The slow cooling rate in current work allow efficient crystal grow for the samples with low basicity (SC1-SC2). That is the reason why the crystal size of the spinel phase increased after slow cooling.

If the element is captured into the lattice of a phase stable to dissolution, the leaching of the element will be negligible. Tanskanen et al. [10] pointed out that Cr leaching from ferrocromium slag is very low despite the fact that the chromium content in the slag is rather high. This apparent contradiction between the high chromium content and the low chromium leaching values from ferrocromium slag was explained by the presence of spinel phase and enclosure of chromium into the glassy phase. Both spinel phase and glass are known to be resistant to dissolution [10]. The glass phase is impermeable and has a high chemical stability[20] Glass can bind a great amount of heavy metals in the amorphous silicatic network structure [21] if formation of continuous Si-O-Si framework is possible[22]. Diffusion

coefficient of an element in the glass phase is low[23]. To optimize the glass formation, Tanskanen et al. suggested rapid cooling. The authors pointed out the significance of the chosen moment of quenching with respect to the crystallization stage. The cooling path before quenching should be sufficiently slow to allow crystallization of spinel[10] . This can only be valid if the basicity of the slag is rather low to allow the glass formation. Results of the current work show that at higher basicities slow cooling is slightly better alternative to rapid cooling. If cooling rate is sufficiently slow Cr dissolved in unstable phases such as merwinite and dicalcium silicate and precipitates as stable to dissolution spinel phase.

The result in current work show that the chromium amount in the soluble and unstable phases decreased after slow cooling. The chromium tends to accumulate in the stable spinel phase; furthermore a stable glass phase is formed on quenching if basicity is low. The exceptions are slags with basicity higher than 1.4, since they are found to contain soluble phases. According to FACTsage calculation, the spinel phase amount is constant, and does not change with temperature in the current basicity and temperature ranges. From the experimental results, however, it is found that the amount of spinel is increased after slow cooling as also the grain size. For example, the presence of Cr_2O_3 dissolved in matrix phases and merwinite at higher temperature and higher basicities imply that this Cr_2O_3 was not available for spinel formation. On cooling, the solubility of Cr_2O_3 in the matrix phases decreased and Cr_2O_3 was rejected from the phase and then could form spinel. The merwinite has started to grow, already at 1873K.

4.2 Effect of the oxygen partial pressure on the chromium partition

Figure 18 shows XRD curves for the samples SC2'-SC4' with basicities in the range 1.2-1.6. The samples were first equilibrated in CO/CO_2 gas mixture at $P_{O_2}=10^{-4}$ Pa 1873 K for 24h, then slow cooled and soaked at 1673 K for additional 24h. Peaks for spinel phase are much more visible than in the previous studies.

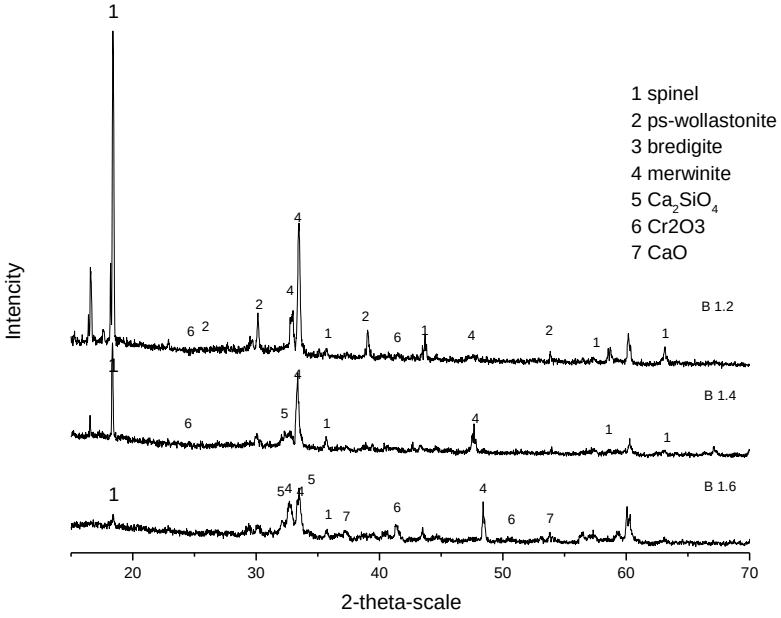

Figure 18 XRD curves for the samples SC2'-SC4' with basicities in the range 1.2-1.6. . The samples were first equilibrated in CO/CO_2 gas mixture at $P_{O_2}=10^{-4}$ Pa 1873 K for 24h, then slow cooled and soaked at 1673 K for additional 24h.

Figure 19 shows the SEM image of the sample SC1' with basicity 1.0. The sample was first equilibrated in CO/CO_2 gas mixture at $P_{O_2}=10^{-4}$ Pa 1873 K for 24h, then slow cooled and soaked at 1673 K for additional 24h. It was observed that the sample remains liquid down to 1673 K. The sample was bright green and transparent. It was found that sample melted completely. Large spinel grains (200 µm) are found, see figure 19. The matrix was found to be amorphous. Cr content in the matrix was less than 0.5 at%, according to EDS analysis see table 14. The amount of impurities dissolved in the spinel phase was also very low <0.5at%. In the Pt – crucible: chromium is evenly distributed and according to EDS analysis is 1.2 at% in all the samples (1.0-1.6). This indicates that equilibrium conditions are fulfilled.

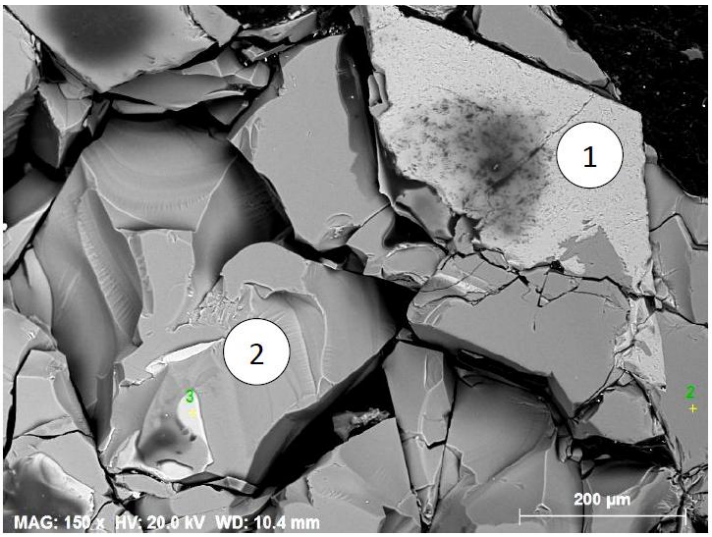

Figure 19 SEM image of the sample SC1'. Large spinel grains with a diameter up to 200µm can be observed.

Notification can be made that the grain size of the spinel phase in not affected by P_{O2}. In comparison with previous study conducted in air by the present authors, the purity of the phases present was found to be improved. The solubility of foreign elements is very low.

Table 14 EDS analysis of the sample S1 (mole%)

	Si	Cr	Ca	Mg	O
1 spinel	0.07	31.40	0.24	12.92	54.47
2 matrix	17.61	0.46	23.34	4.80	53.79

Figure 20 shows SEM micrograph of the sample SC2' with basicity 1.2. The sample was first equilibrated in CO/CO_2 gas mixture at $P_{O_2}=10^{-4}$ Pa 1873 K for 24h, then slow cooled and soaked at 1673 K for additional 24h. It was found that sample was completely melted. The sample was bright green and transparent (amorphous).

Spinel grains, up to 40µm in diameter, can be observed, see figure 20. The matrix consisted of merwenite dendrites and the ps-wollastonite matrix. Bredigite phase was found according to EDS and XRD

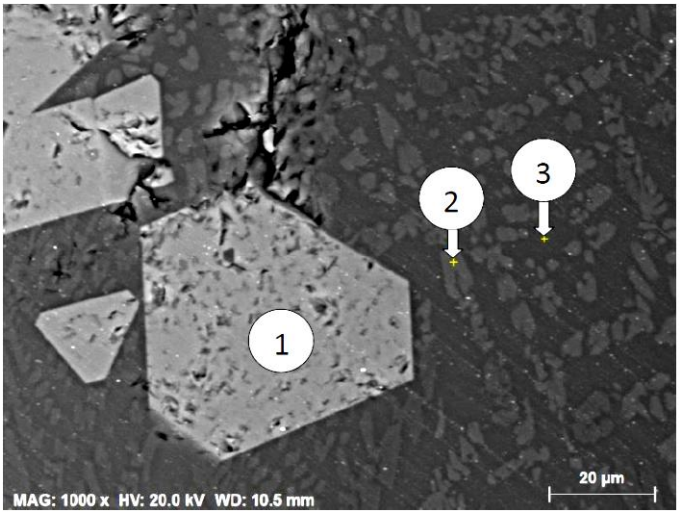

Figure 20 SEM micrograph of the sample SC2' with basicity 1.2 slow cooled to and soaked at 1673K, (1) spinel, the matrix consisted of (2) merwinite dendrites (3) ps-wollastonite

Table 15 EDS analysis of the sample SC2' (mole%)

	Si	Cr	Ca	Mg	O
1 spinel	0.15	34.17	0.46	14.23	50.99
2 merwinite	13.47	0.45	31.96	3.97	50.14
3 ps-wollostonite	17.72	0.40	24.55	3.92	53.41

Figure 21 shows SEM micrograph of the sample SC3' with basicity 1.4. The sample was first equilibrated in CO/CO_2 gas mixture at $P_{O_2}=10^{-4}$ Pa 1873 K for 24h, then slow cooled and soaked at 1673 K for additional 24h. It was found that sample was not melted completely and was gray/green and non transparent in appearance. Fine up to 10µm spinel grains can be observed. The phases present are Ca_2SiO_4, merwinite, spinel; ps-wollastonite and bredigite.

Phases thermodynamically stable at this temperature and composition (sample SC3' basicity 1.4) according to FACTsage calculations are, see table 1; slag liquid, merwinite $Ca_3MgSi_2O_8$, spinel, and a-Ca_2SiO_4. Sample SC3' (basicity 1.4). Figure 18 shows XRD for the sample SC3' with basicity 1.4. According to XRD analysis the sample contained phases spinel, wollastonite, merwinite, Ca_2SiO_4, Cr-Oxide, and $Ca_7Mg(SiO_4)_4$.

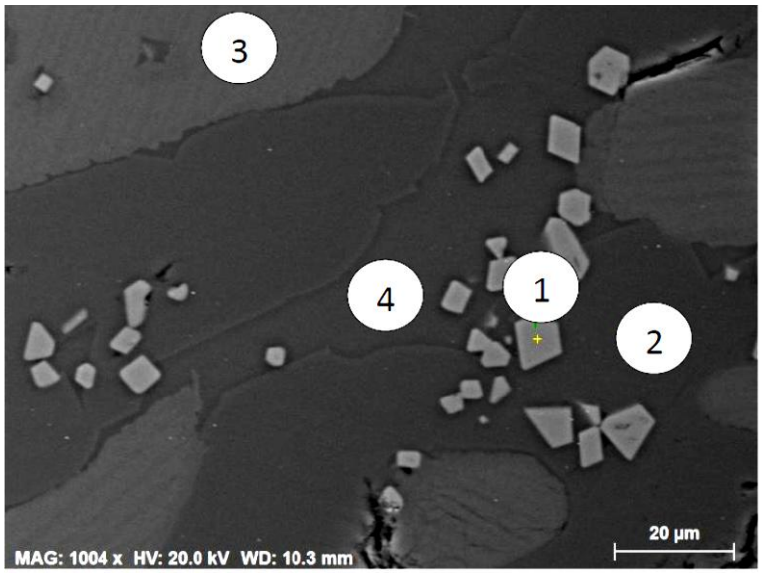

Figure 21 Sample SC3' with basicity 1.4. Fine up to 10µm spinel grains can be observed. SEM micrograph of the sample SC2' with basicity 1.2 slow cooled to and soaked at 1673K, (1) spinel grains up to 200 µm in diameter can be observed. The matrix consisted of (3) ps-wollastonite/bredigete matrix and (4) merwinite dendrites

Table 16 EDS analysis of the sample SC3' (mole%)

	Si	Cr	Ca	Mg	O
1 spinel	-	32.62	1.26	14.07	52.06
2 merwinite	12.99	0.38	29.36	7.75	49.52
3 Ca_2SiO_4	13.22	0.28	35.49	1.71	49.30
4 ps-wollastonite	18.08	0.32	26.30	3.34	51.97

Figure 22 shows SEM micrograph of the sample SC4' with basicity 1.6. The sample was first equilibrated in CO/CO_2 gas mixture at $P_{O_2}=10^{-4}$ Pa 1873 K for 24h, then slow cooled and soaked at 1673 K for additional 24h. It was found that sample was not melted. The shape and high porosity of the sample indicates that the sample remain unmelted (sintered). The color of the sample was gray/green and non transparent. According to SEM/EDS analysis, spinel grains found in large quantities and the phases present are are spinel, Ca_2SiO_4 and $Ca_3MgSi_2O_8$ merwinite. These results are is in good agreement with FACTsage calculations for the sample SC4'. XRD analysis for the sample SC4' (basicity 1.6), see Figure 18, confirmed presence of spinel, merwinite and Ca_2SiO_4. Small amounts of phases periclase, Cr-oxide and $CaMgSi_2O_6$, ps-wollastonite and $Ca_7Mg(SiO_4)_4$ were also detected according to XRD.

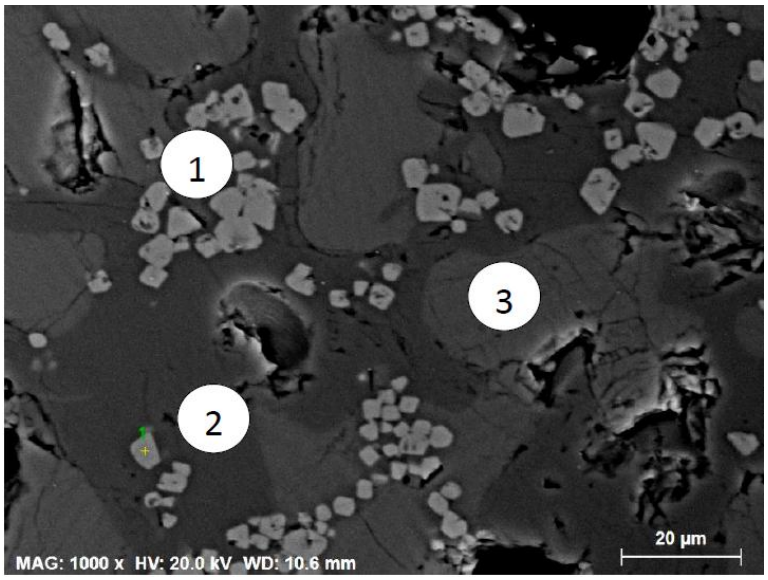

Figure 22 SC4' with basicity 1.6. Spinel grains were found in high quantities. Fine up to 10µm spinel grains can be observed.

Table 17 EDS analysis of the sample S4 (mole %)

	Si	Cr	Ca	Mg	O
1 spinel	0.40	31.66	1.91	12.29	49.17
2 merwinite	14.38	0.29	28.00	7.44	46.56
3 Ca_2SiO_4	14.32	0.32	34.51	2.11	45.34

Figure 23 shows the chromium partition in CaO-SiO_2-MgO-Cr_2O_3 synthetic slag. The results from current work are compared with previous studies of the system. In contrast to results from the samples soaked in air, as shown in the previous articles by current autors [19] the Cr amount in spinel phase is not longer a function of basicity.

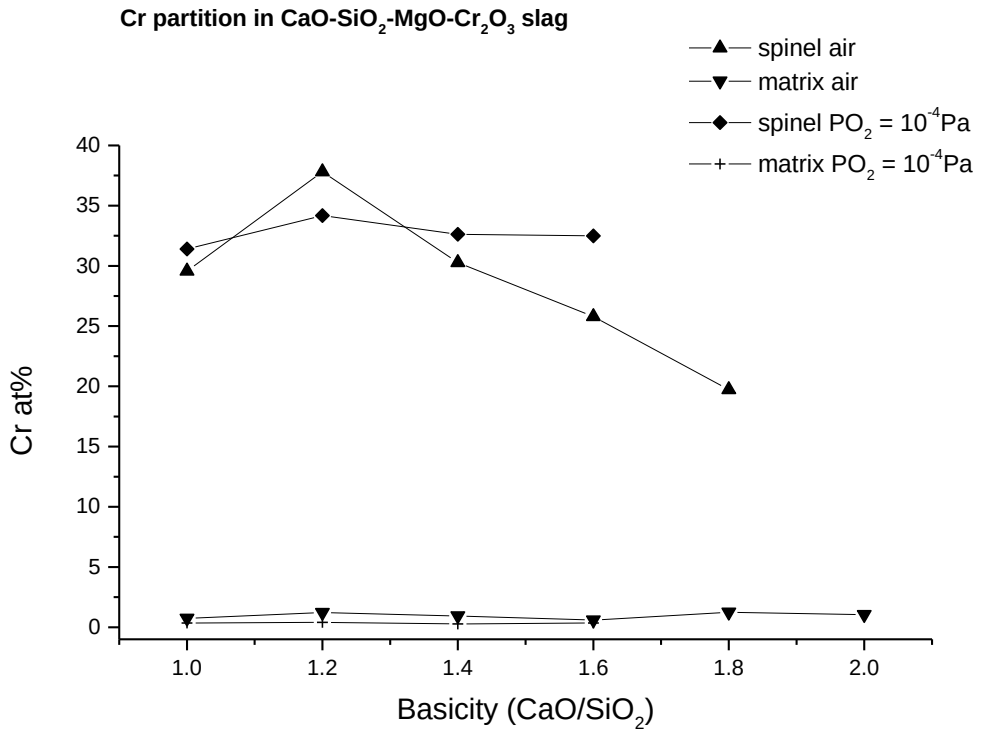

Figure 23 Chromium partition in $CaO\text{-}SiO_2\text{-}MgO\text{-}Cr_2O_3$ synthetic slag. The results from current work are compared with previous studies of the system.

Figure 24 shows activities of liquid CrOx in slag at 1673K in $CaO\text{-}SiO_2\text{-}MgO\text{-}Cr_2O_3$ synthetic slag. The results from current work are compared with previous studies of the system as well as thermodynamic calculations by FACTsage software.

Pengli Dong et al. studied Thermodynamic Activity of Chromium Oxide in $CaO\text{-}SiO_2\text{-}MgO\text{-}Al_2O_3\text{-}CrO_X$ Melts using gas-slag equilibrium technique at very low oxygen partial pressures and elevated temperatures. The activities of CrO decreased with increasing temperature and oxygen partial pressure. If was found that, no significant change of the thermodynamic activity of CrO and the slag basicity could be noticed under the experimental conditions used. The same trend could be observed regarding the CrOx activities in current work. However, a direct comparison is not possible in view of differences in the temperature ranges and compositions used.

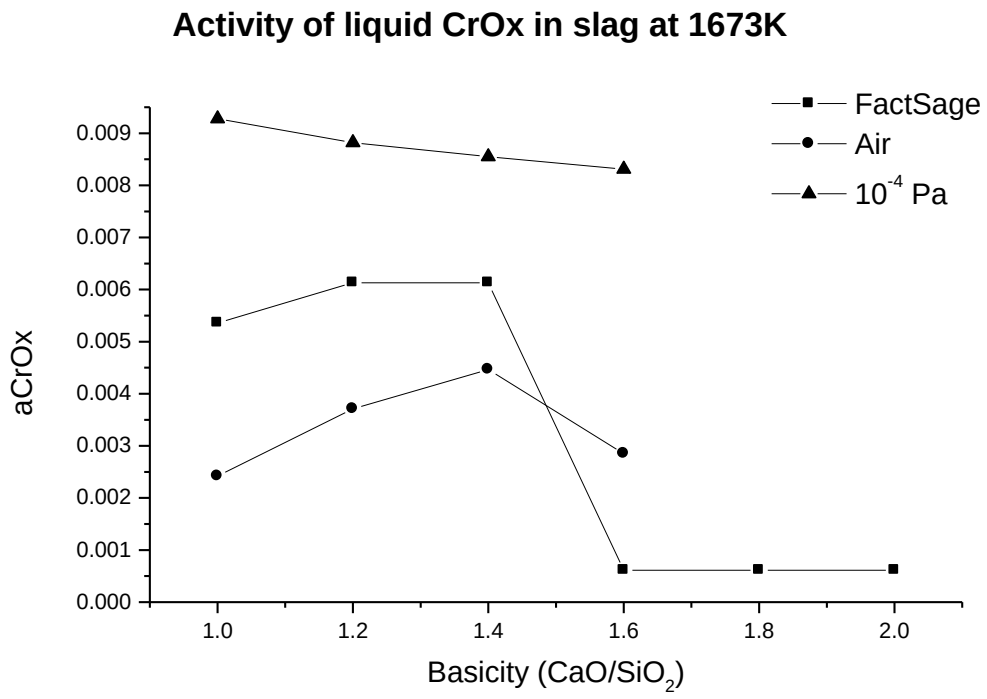

Figure 24 Activity of liquid CrOx in slag at 1673K in $CaO\text{-}SiO_2\text{-}MgO\text{-}Cr_2O_3$ synthetic slag. The results from current work are compared with previous studies of the system as well as thermodynamic calculations by FACTsage software.

It have been shown in earlier studies by current authors [19] that slow cooling enhances the crystal growth of spinel phase and lower the chromium content in the matrix. The purity of the spinel phase precipitated in air atmosphere was found to vary with slag basicity. Slags with basicities above 1.6 contained more Cr distributed in the water soluble matrix phases (merwinate, dicalcium silicate and periclase phases). In the current work, where the experiments were conducted at very low oxygen partial pressure, the chromium partition was no longer dependent on the slag basicity. It was also found that very low P_{O_2} improves the spinel precipitation even at higher basicities. Efficient spinel growth gives very low Cr content in the matrix. The grain size of the spinel crystals can be directly linked to the basicity. It was found that the grain size in the samples SC1'-SC2', with lower basicity (lower melting point) was larger than in sintered (unmelted) samples SC3'-SC4'. Figure 25 illustrates the mean grain size of spinel as a function of basicity. It was also found that low P_{O_2} has a strong impact on the melting temperature of the $CaO\text{-}MgO\text{-}SiO_2\text{-}Cr_2O_3$ slag system. The liquidus temperature increases as P_{O_2}decreases. The grain size of the crystal is controlled by kinetics. Ions in the melt are moving freely, while diffusion in the solid phase can be rather slow compared to the liquid state. The rate of the crystallization process or crystal growth is described and controlled by kinetic laws. Driving force of solidification is proportional to supercooling or supersaturation. The diffusion of atoms or ions in the melt is high compared to solid state and the driving force of spinel formation is high due to cooling. The slow cooling rate in current work allow efficient crystal grow for the samples with low basicity (SC1'-SC2'). It is interesting that the mean grain size of spinel in the sample SC1' is larger

than in the sample SC2'. In the figure 20, merwinite dendrites can be observed surrounded by amorphous matrix. The merwinite dendrites can act as hinder for diffusion of Cr ions through the liquid, thus slowing down the crystal growth of the spinel phase, see figures 20 and 25. For the unmelted samples SC3'-SC4' the crystal size of the spinel phase would be most probably increase if the holding time was increased. However that would, probably not give more volume fraction of spinel, since the Cr amount in the matrix was already extremely low. Tanskanen et al. [4, 10] pointed out that Cr leaching from ferrocromium slag is very low despite the fact that the chromium content in the slag is rather high. This phenomena was explained by the presence of spinel phase and enclosure of chromium into the glassy phase. To optimize the glass formation, Tanskanen et al. suggested rapid cooling. This method can only be valid if the basicity of the slag is relatively low to allow the glass formation. Results of the current work show that at higher basicities slow cooling in combination with low oxygen partial pressure is the only alternative if the slag basicity is relatively high, to avoid the dissolution of harmful element such as Cr in the water soluble matrix phases. The result in current work show that the chromium amount in the soluble and unstable phases decreased after slow cooling. The chromium tends to accumulate in the stable spinel phase; furthermore a stable glass phase is formed on quenching if basicity is low. Improved spinel formation at low oxygen partial pressure cannot be explained by the valence state change of the Cr ions. Chromium exists as Cr^{3+} ion in the spinel phase. The calculations of the ratio Cr^{2+}/Cr^{3+} at the oxygen partial pressure of 10^{-4} Pa, shows however that Cr^{3+} is prevailing in the system, but the Cr^{2+}content has increased compared with results of the samples soaked in air see table 4. Most likely low P_{O_2} is indirectly affecting the CaO activity, since low solubility of the CaO in the spinel phase at lower oxygen partial pressure. At high P_{O_2}, in the samples with high basicity (CaO/SiO_2), CaO enters the spinel phase and thus disturb the crystal growth, since it creates point defects in the crystal structure. Parallels can be drown with other crystals, such as quartz which formation is impossible in the presence of foreign ions. Earlier results by current authors shows that spinel formation is inhibited at higher basicities, which can be explained by presence of CaO dissolved in the spinel phase. In general, the CrOx activity increased with decrease of P_{O_2}, see figure 24. That might make the precipitation of spinel easier.

According to FACTsage calculation, the spinel phase amount is constant, and does not change with temperature in the current basicity and temperature ranges. From the experimental results, however, it is found that the amount of spinel is increased after slow cooling as also the grain size. The reason could be that the FACTsage calculations are based on the assumption that the spinel phase precipitation is completed at higher temperature, and no crystal growth is taking place at lower temperature. FACTsage calculations are not considering the change of P_{O_2} either. One reason for the discrepancies can be that FACTsage lacking data or the experiments have not reached the equilibrium state.

The values given in the table 1, shows that the amount of liquid phase increases as the P_{O_2} decreases according to calculations. This is in contradiction with the experimental results in current work.

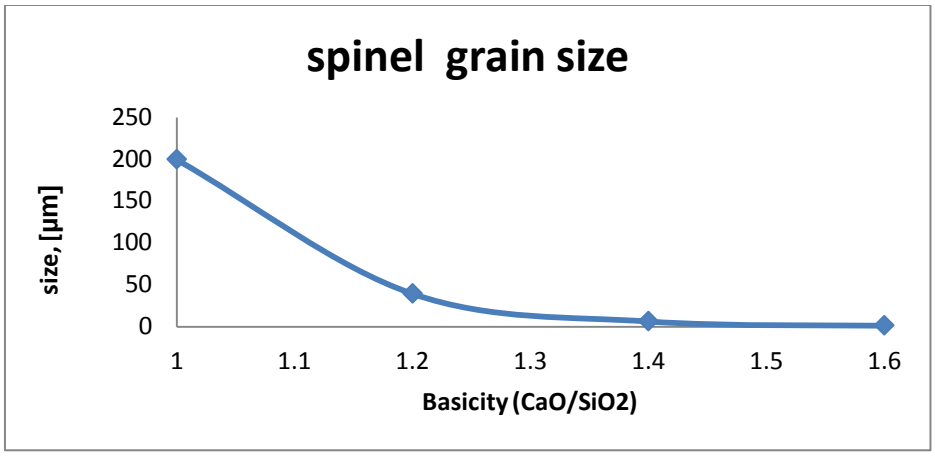

Figure 25 The mean grain size of spinel as a function of basicity.

Chapter 5

Final Discussion and conclusions

The phase correlation in CaO-MgO-SiO_2-Cr_2O_3 slag system in the range of 1673-1873 K has been studied. The Cr_2O_3 and MgO content in the slag were fixed at 6 and 8wt% respectively. The slag basicity was varied in the range of 1.0 to 2.0. Gas/slag equilibrium technique was adopted to synthesize the slags and the equilibration experiments were conducted in air atmosphere as well as at very low oxygen partial pressure. The influence of basicity, heat treatment as well as different oxygen partial pressures on the phase relationships in the CaO-MgO-SiO_2-Cr_2O_3 slags with a view to control the precipitation of Cr-spinel in the slag phase was studied. In low oxygen partial pressure experiments, a suitable mixture of CO and CO_2 was used to control the oxygen partial pressure. The oxygen partial pressure was kept at 10^{-4} Pa. Two different heat treatment procedures were adopted. In the first procedure the samples were heated to and soaked at 1873 K for 24h in order to achieve the equilibrium state and subsequently quenched in water. In the second procedure samples were heated to and soaked at 1873 K for 24h, then slow cooled to 1673 K and soaked at this temperature for additional 24h in order to achieve the equilibrium state before quenching in water. In order to obtain a spinel phase at a temperature of 1873 K (1600 ºC) in air, a slag composition with basicity of around 1.0-1.4 shall be chosen. Higher basicities have to be avoided since it can lead to formation of leacheable chromium containing solid solutions, which are potentially environmentally harmful. The chromium content in the spinel phase is found to decrease with basicity. There are discrepancies between the experimental results and the thermodynamic

calculations by FACTsage software for basicities 1.2 and 1.4, regarding phases wollastonite and merwinite.

The spinel grain size of the spinel phase has increased by one order of magnitude in all samples after slow cooling down to 1673K compared to the samples which were directly quenched from 1873 K. The impurity content (Ca and Si ions) dissolved in the spinel phase is decreased after slow cooling. The amount of the Ca dissolved in the spinel phase, after soaking in air is found to be a function of basisity. Cr content in the matrix decreased after slow cooling as a result of efficient spinel phase growth. Spinel phase has precipitated and grown from merwinite and Ca_2SiO_4 phases on cooling due to low solubility of Cr at lower temperature. The Cr content in the matrix slightly decreased after slow cooling as result of spinel growth. The Cr content in the merwinite dendrites for the sample SC2, basicity 1.2 slightly decreased after slow cooling due to lower solubility of foreign elements at lower temperature. The merwinite phase rejected dissolved chromium oxide into matrix as the temperature decreased. As a result the Cr rejected by merwinite phase was precipapted to form spinel phase in the matrix. The impurity content (Ca and Si ions) dissolved in the spinel phase is decreased drastically after soaking at low P_{O_2} compared with the samples treated in air. Cr content is decreased in the matrix as a result of efficient spinel phase growth. Low P_{O_2} improves the spinel precipitation. P_{O_2} increases the liquidus temperature of CaO-MgO-SiO_2-Cr_2O_3 slag system. The Cr partition is not a function of basicity at low P_{O_2}. At higher basicities and oxygen partial pressures the spinel phase growth is hindered by CaO ions that tend to form solid solutions with MgO and Cr_2O_3. The result is disordered spinel structure. At low P_{O_2} on the other hand the spinel phase has a regular shape.
Slow cooling of slag at low oxygen partial pressure would improve the spinel phase precipitation as well as it will give less Cr dissolved in the soluble matrix phases.

Future work

Steelmaking slags consist of far more elements that covered in current study, thus it would be of interest to investigate the effect of FeO and MnO addition on the chromium partition in the future. I would be particularly interesting to study the effect of Al_2O_3 addition on the chromium partition in slag, since Al_2O_3 addition can theoretically lead to increased spinel amount and thus stabilize Cr in slag.

References

1. F. Engström: Mineralogical Influence of Different Cooling Conditions on Leaching Behaviour of Steelmaking Slag, Doctoral Thesis, Luleå University of Technology, 2010, ISSN: 1402-1544
2. K. Pillay et al.: Ageing of chromium(III)-bearing slag and its relation to the atmospheric oxidation of solid chromium(III)-oxide in the presence of calcium oxide, Chemosphere 52 (2003) 1771–1779.
3. Y. Samada: Prevention of Chromium Elution from Stainless Steel Slag into Seawater, ISIJ International, Vol. 51 (2011), No. 5, pp. 728–73.
4. Gelfi, Cornacchia, Investigations on leaching behavior of EAF steel slags. University of Bresca, Italy, Euroslag 2010, Madrid.
5. T. W. Parker and J. F. Ryder, "Investigations on 'falling' blast furnace slags". Journal of the Iron and Steel Institute, 11, 21-51 (1942)
6. M. Guo, P. Wollants, "EAF stainless steel refining - Part I: Observational study on chromium recovery in an eccentric bottom tapping furnace and a spout tapping furnace". Steel Res. Int., 78 (2) (2007) 117-124.
7. N. Sakamoto, "Effects of MgO based glass addition on the dusting of stainless steel slag (development of control process of stainless steel slag dusting-3)". Current Advance in Materials and Processes, 14 (4) 939 (2001).
8. Q. Yang et al: "Modification study of a steel slag to prevent the slag disintegration after metal recovery and to enhance slag utilisation". In 8th International Conference on Molten Slags, Fluxes and Salts – MOLTEN 2009, 2009, Santiago, Chile.
9. A. Monaco; W-K. Lu: The effect of cooling conditions on the mineralogical characterizations of steel slag, Proc Int Symp Res Conserv Environ Technol Metall Ind, 1994, 107-116
10. P. A. Tanskanen, H. T. Makkonen, Design of Slag Mineralogy and Petrology, University of Oulu, Outocompu Finland, Global Slag Magazine, (5) (2007) 16-20.
11. Wu Ren-Ping; Yu Yan: Influence of Cr_2O_3 on the Structure and Property of Mg-Al Spinel Synthesized by Waste Slag in Aluminium Factory, Chinese J. Struct. Chem. Vol.26, N.12, 1455-1460
12. E. García-Ramos, A. Romero-Serrano, Immobilization of Chromium in Slags using MgO and Al2O3, Steel Research Int. 79 (2008) No. 5, pp 332-339.
13. V. Arredondo-Torres; A. Romero-Serrano: Stabilization of $MgCr_2O_4$ spinel in slags of the SiO_2-CaO-MgO-Cr_2O_3 system, Revista de Metalurgia, 2006, 42 (6) 417-424
14. A. Putnis, Introduction to mineral sciences, pp 137-140, Cambridge. (1992)
15. M. Tossavainen, B. Björkman, "Characteristics of steel slag under different cooling conditions". Waste Management, 27, 1335-1344 (2007)
16. M. Loncnar, A. Jakli, "The effect of water cooling on the leaching behavioue of EAF slag from stainless steel production". Materiali in tehnologije / Materials and technology, 43 (6) 315-321 (2009).
17. Lijun Wang: Experimental and Modelling Studies of the Thermophysical and Thermochemical Properties of Some Slag Systems, Doctoral Thesis, Royal Institute of Technology, 2009.
18. R. J. Choulet: Stainless Steel Refining, (Presented at AISE Seminar on June 5, 1997, in Detroit
19. FactSage software (FactSage 6.1), Thermfact Ltd (Montreal, Canada) and BTT-technologies (Aachen, Germany).
20. E. Pretoris, A. Muan: Activity–Composition Relations in Platinum–Chromium and Platinum–Vanadium Alloys at 1500°C, Journal of the American Ceramic Society, Volume 75, Issue 6, pages 1361–1363, June 1992
21. H. Fredriksson, U. Akerlind: Solidification and Crystalization Processing, Chapter s 9, pp 1-172. Internal publication, Royal Institute of Technology, Casting of Metals (2010)
22. P. Niemel et al.: Production, Characteristics and Use of Ferrochromium Slags, International Ferro-Alloys Congress, New Dehly, (2007)
23. P. Colombo et al. Inertization and reuse of waste materials by vitrification and fabrication of glass-based products, Curr. Opin. Solid State & Mater. Sci., (7) (2003) 225-239.
24. M. Pelino et al. VItrification of Electric Arc Furnace Dust. Waste Management, 22, (2002) 245-949
25. H. I. Inyang: Framework for Recycling of Wastes in Construction, Journal of Enviromental Engineering. 129 (2003) 887-898.